Robustness of time reversal versus all-rake transceivers in multiple access channels

Hindawi
Wireless Communications and Mobile Computing
Volume 2018, Article ID 7548926, 16 pages
https://doi.org/10.1155/2018/7548926

Research Article

Robustness of Time Reversal versus All-Rake Transceivers in Multiple Access Channels

Luca De Nardis,[1] **Jocelyn Fiorina**,[2] **Guido Carlo Ferrante**,[3] **and Maria-Gabriella Di Benedetto**[1]

[1]*Department of Information Engineering, Electronics and Telecommunications, Sapienza University of Rome, Rome, Italy*
[2]*Laboratoire des Signaux et Systèmes (L2S), CentraleSupélec-CNRS-Université Paris-Sud, Université Paris-Saclay, 3, rue Joliot Curie, 91192 Gif-sur-Yvette, France*
[3]*Department of Electrical Engineering, Chalmers University of Technology, Gothenburg, Sweden*

Correspondence should be addressed to Luca De Nardis; luca.denardis@uniroma1.it

Received 31 December 2017; Revised 29 March 2018; Accepted 7 May 2018; Published 11 June 2018

Academic Editor: Simone Morosi

Time reversal (TR) is an effective solution in both single user and multiuser communications for moving complexity from the receiver to the transmitter, in comparison to traditional postfiltering based on Rake receivers. Imperfect channel estimation may, however, affect pre- versus postfiltering schemes in a different way; this paper analyzes the robustness of time reversal versus All-Rake (AR) transceivers, in multiple access communications, with respect to channel estimation errors. Two performance indicators are adopted in the analysis: symbol error probability and spectral efficiency. Analytic expressions for both indicators are derived and used as the basis for simulation-based performance evaluation. Results show that while TR leads to slight performance advantage over AR when channel estimation is accurate, its performance is severely degraded by large channel estimation errors, indicating a clear advantage for AR receivers in this case, in particular when extremely short impulsive waveforms are adopted. Results however also show a stronger non-Gaussianity of interference in the TR case suggesting that the adoption of a receiver structure adapted to non-Gaussian interference might tilt the balance towards TR.

1. Introduction

Time reversal (TR) is a signal processing technique that takes advantage of the field equivalence principle [1–4] and was originally proposed in acoustics [5–7]. By prefiltering transmissions with a scaled version of the channel impulse response, reversed in time, TR allows simplification of receiver design, since the channel is compensated by precoding at the transmitter and can simplify the task of synchronization at the transmitter.

In a legacy network, e.g., 3G or WiFi, where Base Stations (BS) or Access Points (APs) were typically characterized by higher computational power, TR would be typically implemented in downlink, in order to concentrate most of the complexity on the network side. However, the evolution of networks is leading more and more to use cases where devices with identical characteristics can play different roles at different times, as for example in Device-2-Device (D2D) connections that are already planned in LTE and are expected to become common in 5G networks [8]. This is particularly true in light of the extremely high density of devices and, in turn, of massive amount of data expected in 5G networks, that will call for efficient data fusion and data concentration techniques [9], where in turn one device will take the responsibility of collecting and merging the data generated by a large number of other devices. In such a use case, moving the complexity on the device that is playing the role of sink/data collector is not necessarily the optimal choice and in some cases might not even be feasible. In this context, this work focuses on the analysis of what happens at the sink when comparing two approaches: TR, where the complexity is distributed among devices, versus AR, where the complexity is concentrated at the BS, taking care of compensating the impact of the channels for all links. In agreement with such use case scenario identified above, the network model in this work, shown in Figure 1, considers multiple access by K user

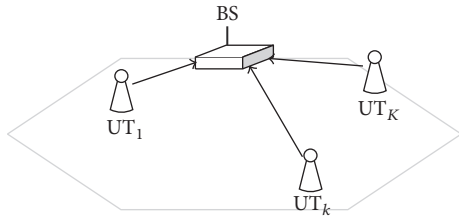

Figure 1: Network model: several user terminals (UTs) transmit information-bearing symbols to a common sink, i.e., base station (BS).

terminals (UTs) communicating to one BS, where UTs and BS differ in their functional roles (sources versus sink), but not in general in their hardware characteristics.

Pioneering work on single-antenna TR spread-spectrum communications dates back to the nineties, where the TR prefilter was named *pre-Rake* [10, 11]. The basic idea was to prefilter the transmitted pulse with the channel impulse response reversed in time, therefore matching the transmitted signal with the subsequent channel.

Precoding techniques for multiuser spread-spectrum systems were developed along similar lines of receive filters: transmit Zero-Forcing (ZF) [12], that attempts to preequalize the channel by flattening the effective channel formed by the cascade of the prefilter and the actual channel, is optimum in the high-SNR regime; transmit matched filter (MF), that has been recognized to be equivalent to the pre-Rake filter in [13], conversely is optimum in the low-SNR regime; and finally, transmit MMSE (Wiener) filter minimizing the SINR was derived in [14] following previous attempts [15, 16].

In recent years, along with the fast developing of narrowband MIMO systems, precoding techniques using multiple antennas at the transmitter were thoroughly studied (for a complete overview on MIMO precoding; see [17]). Since the mathematical formulation of multiuser spread-spectrum is very close to that of MIMO communications (see [18] for an overview of this analogy), MIMO linear precoders can be derived along similar techniques. Significant research efforts were then devoted to the analysis of the impact of imperfect channel estimation on such systems, with several authors proposing closed-formulas for BER evaluation in both SISO and MIMO systems affected by channel estimation errors [19–22].

TR was proposed in connection with UWB communications in [23] that also addressed equalization through an MMSE receiver. In [24], early experimental data, showing the feasibility of TR, were collected. Shortly after, experimental investigations on multiple-antenna systems with TR [25–27] and performance analyses [28] were also pursued. In [29, 30], compensation for pulse distortion in connection with TR was investigated. In [31], the trade-off between the complexity of transmitter versus receiver in terms of number of paths was analyzed. In [32], the robustness of TR to the lack of correlation between channels in a MISO system was investigated. Finally, in [33], the effect of TR on statistical properties of multiuser interference in communication versus positioning was explored.

The above investigations were all carried out based on the hypothesis of perfect channel estimation. Only recently, the impact of imperfect channel state information (CSI) on the performance of TR was experimentally investigated in the case of UWB signals in [34], and analytic expressions for BER evaluation in a TR-UWB system in presence of channel estimation errors were provided in [35], where an iterative algorithm to compensate for estimation errors was also proposed. The impact of a channel estimation error in a TR-UWB system was analyzed in terms of Bit Error Probability also in [36], focusing however only on BPSK modulation, and in [37], where an uncoordinated network of IR-UWB devices was considered. The impact of nonstationarity in the channel on TR-UWB communications was addressed in [38], comparing a TR and a conventional system in terms of BER and mutual information assuming that the error is determined by temporal variation in the channel coefficients and carrying thus out the analysis as a function of the correlation coefficient ρ between real and estimated channel. The impact of channel nonstationarity was also addressed in [39], and the analysis was extended in [40] by considering the combined impact of nonstationarity and channel coefficients quantization in terms of BER.

The above works highlighted that channel estimation errors, in particular due to nonstationarity, may affect the performance of TR systems, although the actual impact mainly depends on the degree of stationarity of the channel. Several aspects are however still open: in particular, an exhaustive comparison of how channel estimation error affects TR in comparison to other techniques; e.g., receiver-based schemes is still missing, and the impact of imperfect CSI in presence of Multiple User Interference (MUI) was only partially addressed.

This paper investigates such issues, focusing on the specific case of single-antenna UWB systems using TR versus as an exemplary case of a receiver-based scheme, that is an AR scheme. The contributions of this paper can be thus identified as follows:

(i) It carries out an extensive comparison of TR versus AR under imperfect CSI, not carried out to this extent in the previous works on this topic, and adopts an estimation error model more general than the use of correlation coefficient adopted in most of such works.

(ii) It derives mutual information for TR versus AR schemes in presence of both CSI estimation error and MUI.

(iii) It analyzes the statistical properties of MUI in order to provide hints on how such properties might be used to improve the performance of a TR system under imperfect CSI.

Comparison of performance of TR versus AR transceivers will be carried out in terms of effect of imperfect channel state information (CSI) on symbol error probability of a generic information-bearing symbol for a given UT (see [41] for a work adopting a similar approach in other systems, in particular CDMA). The analysis will further explore robustness of TR versus AR, by finding the maximum achievable rate for

the uplink channel. Finally, the maximum information rate, that takes into account channel estimation overhead, will be explored.

The paper is organized as follows: Section 2 contains the reference model; Section 3 is devoted to the performance analysis in terms of symbol error probability, while Section 4 presents the comparison between TR and AR in terms of uplink rate as measured by the mutual information. Finally, Section 5 contains the conclusions.

2. Reference Model

This section is organized as follows: Section 2.1. *System model*; Section 2.2. *Single User Channel*; Section 2.3. *Multiuser Channel*; Section 2.4. *Channel Estimation and Data Transmission*.

2.1. System Model. A generic UT_k transmits data that is encoded into a sequence of information-bearing symbols $\{b_k[m] : m \in \mathbb{Z}\}$. This set of symbols is partitioned into blocks of n symbols each, $\{\mathbf{b}_k[i] : i \in \mathbb{Z}\}$ where $\mathbf{b}_k[i] = (b_k[in], \ldots, b_k[(i+1)n-1])^{\mathsf{T}}$, where the length n of the block is typically determined based on the coherence time T_{coh} of the channel. Each block is transmitted by using the following signal:

$$s_{k,i}\left(t; \mathbf{b}_k[i]\right) = \sum_{m=in}^{(i+1)n-1} b_k[m]\, \mathrm{g}_{k,m}\left(t - mT_{\mathrm{s}}\right), \tag{1}$$

where T_{s} (sec) is the symbol period and $\mathrm{g}_{k,m}(t)$ is the unit energy waveform associated with the m-th symbol of user k. In general, $\mathrm{g}_{k,m}(t)$ is a spread-spectrum signal at user k prefilter output and has band $[-\mathsf{W}/2, \mathsf{W}/2]$; that is, its spectrum is nonzero for $|f| \leq \mathsf{W}/2$. Assuming that $\{\mathrm{g}_{k,m}(t - mT_{\mathrm{s}}) : m = in, \ldots, (i+1)n-1\}$ are orthonormal, or very mildly cross-correlated, the energy of $s_{k,i}(t; \mathbf{b}_k[i])$ in (1) is $n\mathbb{E}[|b_k[m]|^2]$; since the block has duration nT_{s}, the average power is $\mathscr{P}_k = \mathbb{E}[|b_k[m]|^2]/T_{\mathrm{s}}$.

In the adopted model, demodulation at BS is performed on a block-by-block basis. Index i, that specifies the block number, can be thus dropped. Consider for the sake of simplicity $i = 0$ in (1):

$$s_k\left(t; \mathbf{b}_k\right) = \sum_{m=0}^{n-1} b_k[m]\, \mathrm{g}_{k,m}\left(t - mT_s\right). \tag{2}$$

Figure 2 shows the system model, including K modulators producing K transmitted signals, $s_k(t)$, $k = 1, \ldots, K$, affected by propagation within K different channels and corrupted at the receiver by white Gaussian noise $n(t)$. The receiver consists in one demodulator.

Transmitted signal $s_k(t; \mathbf{b}_k)$ of each user propagates over a multipath channel with impulse response $c_k(t)$ leading to the signal $x_k(t)$:

$$x_k\left(t; \mathbf{b}_k\right) = s_k\left(t; \mathbf{b}_k\right) * c_k\left(t\right) = \sum_{\ell=0}^{\infty} c_{k,\ell}\, s_k\left(t - \tau_{k,\ell}; \mathbf{b}_k\right), \tag{3}$$

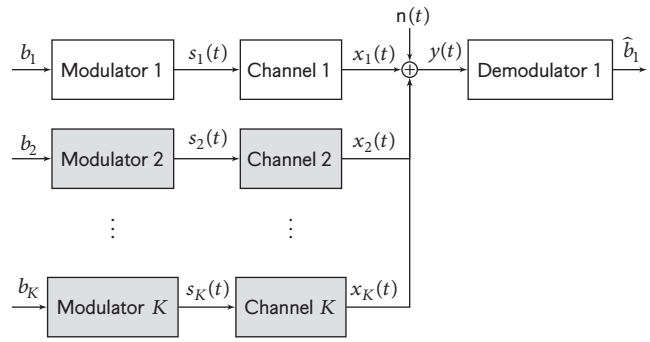

Figure 2: System model. The transmitter is formed by K modulators, representing the K UTs. Radiated signals are affected by K different channels and white Gaussian noise $n(t)$ at the receiver. Receiver consists in one demodulator shown on the figure for the example case of user 1.

where $\{c_{k,\ell} : \ell \geq 0\}$ and $\{\tau_{k,\ell} : \ell \geq 0\}$ are amplitudes and delays of the paths of $c_k(t)$, respectively. The received signal is as follows:

$$y\left(t; \mathbf{b}\right) = \sum_{k=1}^{K} x_k\left(t; \mathbf{b}_k\right) + n\left(t\right), \tag{4}$$

where $n(t)$ is a white Gaussian noise with flat power spectral density $\mathscr{N}_0/2$ (W/Hz).

Throughout the paper it is assumed that the receiver estimates transmitted symbols of user k, $\{b_k[m] : k = 1, \ldots, K; m = 0, \ldots, n-1\}$, on a symbol-by-symbol basis, by considering users $j \neq k$ as unknown interference over user k; for example, Figure 2 shows the demodulation of user 1. As detailed below, transmissions are symbol-synchronous but not necessarily chip-synchronous; therefore the symbol-by-symbol demodulation does not imply any performance loss. In the adopted model, in agreement with the scenario defined in Section 1, the receiver is a single user detector and as such suboptimal, since it does not take into account the possibility of joint multiuser detection, which is left for future work. In addition, throughout the paper it is assumed that the transmission data rate is such that Intersymbol Interference (ISI) is negligible in agreement with other works operating under the same assumption in the literature; see, for example, [38, 39].

How channel is estimated and how errors in channel estimation play a role in the model will be explained later in this section, in association with the different modulation and demodulation structures. Considering signals for the symbol at time epoch $m = 0$, notation can be simplified by setting $b_k = b_k[0]$, and (2), (3), and (4) become the following:

$$s_k\left(t; b_k\right) = b_k \mathrm{g}_{k,0}\left(t\right), \tag{5}$$

$$\begin{aligned} x_k\left(t; b_k\right) &= s_k\left(t; b_k\right) * c_k\left(t\right) \\ &= \sum_{\ell=0}^{\infty} c_{k,\ell}\, s_k\left(t - \tau_{k,\ell}; b_k\right), \end{aligned} \tag{6}$$

$$y(t; b_1, \ldots, b_K) = \sum_{k=1}^{K} x_k(t; b_k) + n(t). \quad (7)$$

2.2. Single User Channel. Since the system is symbol-synchronous, analysis may refer to transmission of one generic symbol, that is chosen as symbol $m = 0$; the index k can be dropped in order to simplify the notation, leading to $b[0] = b$, $g_0(t) = g_{k,0}(t)$.

If transmission does not foresee prefiltering, that is, a zero-excess bandwidth pulse $\psi(t)$ with bandwidth W and unit energy is transmitted to modulate b, the received signal is as follows:

$$\begin{aligned} y(t; b) &= x(t; b) + n(t) = b g_0(t) * c(t) + n(t) \\ &= b \sum_{\nu=0}^{N-1} \mathsf{s}[\nu]\, \psi(t - \nu T_c) * c(t) + n(t) \end{aligned} \quad (8)$$

where the spreading sequence $\mathbf{s} = (\mathsf{s}[0], \ldots, \mathsf{s}[N-1])^{\mathsf{T}}$ and the chip period T_c are made explicit. In the following, time-hopping is considered, for which all $\mathsf{s}[\nu]$ are zero, but one.

Since $\psi(t)$, and therefore also $\psi(t) * c(t)$, are bandlimited to $\mathsf{W}/2$, these signals can be represented by their samples spaced by $T = 1/\mathsf{W}$; in particular, $c(t)$ will be represented by its samples $c[l] = c(l/\mathsf{W})$, $l = 0, \ldots, +\infty$. One has thus the following:

$$y(t; b) = b \sum_{\nu=0}^{N-1} \mathsf{s}[\nu] \sum_{\ell=0}^{+\infty} c[\ell]\, \psi\left(t - \frac{\ell}{\mathsf{W}} - \nu T_c\right) + n(t). \quad (9)$$

In general, one will have $T_c \leq T = 1/\mathsf{W}$, where the case $T_c > T$ corresponds to a pulse duration shorter than chip duration, as common in UWB communications. This is taken into account in the model by defining the *impulsiveness index* $\dot{\iota}$, a positive integer defined such that $T_c = \dot{\iota}/\mathsf{W}$; note that $\dot{\iota}$ can be equivalently interpreted as the number of samples per chip time T_c. Furthermore it can be safely assumed that the channel impulse response $c(t)$ is causal and has finite delay spread T_d. By introducing the approximation $T_d \approx LT_c = L\dot{\iota}/\mathsf{W}$, where L is an integer, one has $c[\ell] = 0$ for $\ell < 0$ and $c[\ell] = 0$ for $\ell > L\dot{\iota}$. As a result, one can write the following:

$$y(t; b) = b \sum_{\nu=0}^{N-1} \mathsf{s}[\nu] \sum_{\ell=0}^{L\dot{\iota}} c[\ell]\, \psi\left(t - \frac{(\ell + \nu\dot{\iota})}{\mathsf{W}}\right) + n(t), \quad (10)$$

By projecting (10) onto $\{\psi(t - k/\mathsf{W}) : k = 0, \ldots, (N+L+1)\dot{\iota} - 1 - 1\}$, the following discrete model is obtained:

$$\mathbf{y} = \mathbf{C}\mathbf{x}b + \mathbf{n}, \quad \mathbf{x} = \mathbf{s} \otimes \mathbf{e}_1^{\dot{\iota}}, \quad (11)$$

where the symbol $\otimes$ indicates the Kronecker product, $\mathbf{e}_1^{\dot{\iota}} = [1, \mathbf{0}_{(\dot{\iota}-1)\times 1}^{\mathsf{T}}]^{\mathsf{T}}$ is the first vector of the canonical basis of $\mathbb{R}^{\dot{\iota}}$, $\mathbf{x}$ is $N\dot{\iota} \times 1$, and $\mathbf{C}$ is a banded Toeplitz matrix with dimensions $(N + L + 1)\dot{\iota} - 1 \times N\dot{\iota}$ and elements $C_{ij} = c[i - j]$.

In general, for a system with prefiltering, with prefiltering impulse response $p(t)$, (11) generalizes to the following (see, e.g., [18]):

$$\mathbf{y} = \mathbf{C}\mathbf{P}\mathbf{x}b + \mathbf{n}, \quad (12)$$

where $\mathbf{P}$ is a Toeplitz matrix with dimensions $(N+2L)\dot{\iota} \times (N + L + 1)\dot{\iota} - 1$ and elements $P_{ij} = p[i - j] = p * \psi((i - j)/\mathsf{W})$.

In this paper, prefiltering is introduced in order to compensate channel effects; in particular, prefiltering is based on an estimated version of the channel impulse response. In other words, imperfect prefiltering may be matched to channel estimation error patterns. If prefiltering is imperfect, as will be justified in Section 2.4, the error due to the estimation process can be modeled as a white Gaussian process $\xi(t)$, that is, added to $\mathbf{P}$ as follows [42]:

$$\widehat{\mathbf{P}} = \alpha(\mathbf{P} + \Xi), \quad (13)$$

where $\Xi_{ij} = \xi_{i-j} \sim \mathcal{N}(0, \sigma_\xi^2)$, where σ_ξ^2 accounts for estimation accuracy, and $\alpha > 0$ is such that $\|\widehat{\mathbf{P}}\mathbf{x}\|^2 = \|\mathbf{P}\mathbf{x}\|^2$, so as to ensure an equal energy comparison.

No Prefiltering, All-Rake Receiver. The traditional (or conventional) receiver is a matched filter, i.e., an AR receiver in the case of a multipath channel. Knowing the time-hopping spreading sequence $\mathbf{x}$ and the resolved channel $\mathbf{c}$, a sufficient statistic for b is obtained by projecting the received signal $\mathbf{y}$ onto $\mathbf{h} = \mathbf{C}\mathbf{x}$, or, equivalently, onto $\mathbf{h}/\|\mathbf{h}\|$:

$$z^{\mathrm{AR}} = \frac{\mathbf{h}^{\mathsf{T}}}{\|\mathbf{h}\|}\mathbf{y} = \|\mathbf{h}\|\, b + \nu, \quad (14)$$

where $\nu \sim \mathcal{N}(0, \mathcal{N}_0/2)$.

As occurs in the prefiltering, also the AR receiver is affected by possible channel estimation errors. If the AR receiver is provided with imperfect CSI, that is, operates using an estimation $\widehat{\mathbf{c}}$ of channel $\mathbf{c}$ that is impaired by an error $\boldsymbol{\chi} \sim \mathcal{N}(\mathbf{0}, \sigma_\xi^2 \mathbf{I}_{(L\dot{\iota}+1)})$, then it combines paths through $\widehat{\mathbf{h}} \triangleq \widehat{\mathbf{C}}\mathbf{x}$ instead of $\mathbf{h} = \mathbf{C}\mathbf{x}$, and inference of b is based on the following:

$$\begin{aligned} \widehat{z}^{\mathrm{AR}} &= \frac{\widehat{\mathbf{h}}^{\mathsf{T}}}{\|\widehat{\mathbf{h}}\|}\mathbf{y} = \frac{(\mathbf{h} + \boldsymbol{\chi})^{\mathsf{T}}}{\|\mathbf{h} + \boldsymbol{\chi}\|}(\mathbf{h}b + \mathbf{n}) \\ &= \frac{(\mathbf{h} + \boldsymbol{\chi})^{\mathsf{T}}}{\|\mathbf{h} + \boldsymbol{\chi}\|}\mathbf{h}b + \frac{(\mathbf{h} + \boldsymbol{\chi})^{\mathsf{T}}}{\|\mathbf{h} + \boldsymbol{\chi}\|}\mathbf{n}, \end{aligned} \quad (15)$$

where $\boldsymbol{\chi} = [\mathbf{0}_{j_{\mathbf{x}}}^{\mathsf{T}}, \boldsymbol{\xi}^{\mathsf{T}}, \mathbf{0}_{N\dot{\iota}-j_{\mathbf{x}}}^{\mathsf{T}}]^{\mathsf{T}}$, $j_{\mathbf{x}}$ being the nonzero dimension of $\mathbf{x}$.

TR Prefiltering, 1Rake Receiver. The TR prefilter is represented by $p[j] = \alpha c[L\dot{\iota} - j]$, where $\alpha > 0$ guarantees that prefiltered and non-prefiltered transmitted waveforms have same energy. Time-hopping implies $\mathbf{s} \in \{\mathbf{e}_\nu\}_{\nu=1}^{N}$, and $\mathbf{x} = \mathbf{s} \otimes \mathbf{e}_1^{\dot{\iota}} \in \{\mathbf{e}_{(\nu-1)\dot{\iota}+1}\}_{\nu=1}^{N}$. A 1Rake receiver is given by $\mathbf{e}_{L\dot{\iota}+j_{\mathbf{x}}}$. Denoting by $\mathbf{T}$ the TR prefilter matrix, one has the following:

$$\begin{aligned} z^{\mathrm{TR}} &= \mathbf{e}_{L\dot{\iota}+j_{\mathbf{x}}}^{\mathsf{T}}\mathbf{y} = \mathbf{e}_{L\dot{\iota}+j_{\mathbf{x}}}^{\mathsf{T}}\mathbf{C}\mathbf{T}\mathbf{x}b + \mathbf{e}_{L\dot{\iota}+j_{\mathbf{x}}}^{\mathsf{T}}\mathbf{n} \\ &= \mathbf{e}_{L\dot{\iota}+j_{\mathbf{x}}}^{\mathsf{T}}\mathbf{H}\mathbf{x}b + n_{L\dot{\iota}+j_{\mathbf{x}}}, \end{aligned} \quad (16)$$

being $n_{L\dot{\iota}+j_{\mathbf{x}}} \sim \mathcal{N}(0, \mathcal{N}_0/2)$ and having defined $\mathbf{H} = \mathbf{C}\mathbf{T}$.

If the transmitter is provided with imperfect CSI, then model of (13) holds, and (16) becomes the following:

$$\begin{aligned}\widehat{z}^{\mathrm{TR}} &= \mathbf{e}_{L\dot{\imath}+j_{\mathbf{x}}}^{\mathsf{T}}\mathbf{C}\widehat{\mathbf{T}}\mathbf{x}b + \mathbf{e}_{L\dot{\imath}+j_{\mathbf{x}}}^{\mathsf{T}}\mathbf{n} \\ &= \mathbf{e}_{L\dot{\imath}+j_{\mathbf{x}}}^{\mathsf{T}}\mathbf{C}\left[\alpha\left(\mathbf{T}+\Xi\right)\right]\mathbf{x}b + n_{L\dot{\imath}+j_{\mathbf{x}}}.\end{aligned} \tag{17}$$

AR versus TR. As well-known [33], TR is equivalent to a system without prefiltering and AR in terms of the signal-to-noise ratio. From a single user perspective, there is no performance difference in both uncoded (symbol error probability) and coded (channel capacity) regimes between the two transceiver structures. Moreover, previous work [31] suggested that sets of equivalent systems can be obtained with partial Rakes compensating for partial TR transmitter structures. This paper extends the comparison of AR versus TR to the case where imperfect CSI is available.

2.3. Multiuser Channel. A straightforward extension of (11) to K users is as follows:

$$\mathbf{y} = \sum_{k=1}^{K}\mathbf{C}_k\mathbf{x}_k b_k + \mathbf{n}, \tag{18}$$

where $\mathbf{x}_k = \mathbf{s}_k \otimes \mathbf{e}_{l_k}^{\dot{\imath}}$ and $1 \le l_k \le \dot{\imath}$ models the chip-asynchronism by making l_k i.i.d. according to a uniform distribution. This extension holds based on the hypothesis that all UTs are symbol-synchronous. This hypothesis is reasonable since, as further discussed in Section 2.4, the BS broadcasts in a link setup phase a known sequence to the UTs.

Denoting by $\mathbf{h}_k = \mathbf{C}_k\mathbf{x}_k$ the spreading sequence $\mathbf{x}_k$ after transition in the multipath channel, and by

$$\mathbf{H} = \sum_{k=1}^{K}\mathbf{e}_k^{\mathsf{T}} \otimes \mathbf{h}_k = \left[\mathbf{h}_1, \ldots, \mathbf{h}_K\right] \tag{19}$$

the spreading matrix, (11) can also be rewritten as follows:

$$\mathbf{y} = \mathbf{H}\mathbf{b} + \mathbf{n}, \tag{20}$$

where $\mathbf{b} = (b_1, \ldots, b_K)^{\mathsf{T}}$.

For systems with prefiltering, (18) generalizes to

$$\mathbf{y} = \sum_{k=1}^{K}\mathbf{C}_k\mathbf{P}_k\mathbf{x}_k b_k + \mathbf{n}, \tag{21}$$

where matrices $\mathbf{P}_k$ and $\mathbf{C}_k$ have same dimensions as $\mathbf{P}$ and $\mathbf{C}$ of (12), respectively, and (20) holds with $\mathbf{h}_k = \mathbf{C}_k\mathbf{P}_k\mathbf{x}_k$.

In the presence of imperfect CSI, $\mathbf{P}_k$ in (21) is substituted by $\widehat{\mathbf{P}}_k$, as defined in (13), where estimation errors are independent of k.

No Prefiltering, All-Rake Receiver. The decision variable following the matched filter of user k is

$$\begin{aligned}z_k^{\mathrm{AR}} &= \left\|\mathbf{h}_k\right\| b_k + \sum_{\substack{j=1\\ j\neq k}}^{K}\frac{\mathbf{h}_k^{\mathsf{T}}}{\left\|\mathbf{h}_k\right\|}\mathbf{h}_j b_j + \frac{\mathbf{h}_k^{\mathsf{T}}}{\left\|\mathbf{h}_k\right\|}\mathbf{n} \\ &= \left\|\mathbf{h}_k\right\| b_k + I_k + \nu_k,\end{aligned} \tag{22}$$

where $\mathbf{h}_i = \mathbf{C}_i\mathbf{x}_i$, I_k represents the MUI and $\nu_k = (\mathbf{h}_k^{\mathsf{T}}/\|\mathbf{h}\|)\mathbf{n} \sim \mathcal{N}(0, \boldsymbol{\mathcal{N}}_0/2)$.

If the AR is provided with imperfect CSI, then signal $\mathbf{y}$ is projected onto $\widehat{\mathbf{h}}_k$ instead of $\mathbf{h}_k$, hence

$$\begin{aligned}\widehat{z}_k^{\mathrm{AR}} &= \frac{\widehat{\mathbf{h}}_k^{\mathsf{T}}}{\left\|\widehat{\mathbf{h}}_k\right\|}\mathbf{h}_k b_k + \sum_{\substack{j=1\\ j\neq k}}^{K}\frac{\widehat{\mathbf{h}}_k^{\mathsf{T}}}{\left\|\widehat{\mathbf{h}}_k\right\|}\mathbf{h}_j b_j + \frac{\widehat{\mathbf{h}}_k^{\mathsf{T}}}{\left\|\widehat{\mathbf{h}}_k\right\|}\mathbf{n} \\ &= \widehat{a}_{kk}^{\mathrm{AR}} b_k + \widehat{I}_k^{\mathrm{AR}} + \widehat{\nu}_k^{\mathrm{AR}},\end{aligned} \tag{23}$$

where $\widehat{\nu}_k^{\mathrm{AR}} = (\widehat{\mathbf{h}}_k^{\mathsf{T}}/\|\widehat{\mathbf{h}}_k\|)n \sim \mathcal{N}(0, \boldsymbol{\mathcal{N}}_0/2)$.

TR Prefiltering, 1Rake Receiver. With TR, the decision variable for user k becomes the following:

$$z_k^{\mathrm{TR}} = \mathbf{e}_{q_k}^{\mathsf{T}}\mathbf{C}_k\mathbf{T}_k\mathbf{x}_k b_k + \sum_{\substack{j=1\\ j\neq k}}^{K}\mathbf{e}_{q_k}^{\mathsf{T}}\mathbf{C}_j\mathbf{T}_j\mathbf{x}_j b_j + \mathbf{e}_{q_k}^{\mathsf{T}}\mathbf{n}, \tag{24}$$

where $q_k = L\dot{\imath} + j_{\mathbf{x}_k}$ is the delay (in samples) to which the 1Rake is synchronized. In the presence of imperfect CSI, the decision variable is

$$\begin{aligned}\widehat{z}_k^{\mathrm{TR}} &= \mathbf{e}_{q_k}^{\mathsf{T}}\mathbf{C}_k\alpha_k\left(\mathbf{T}_k + \Xi_k\right)\mathbf{x}_k b_k \\ &\quad + \sum_{\substack{j=1\\ j\neq k}}^{K}\alpha_j\mathbf{e}_{q_k}^{\mathsf{T}}\mathbf{C}_j\left(\mathbf{T}_j + \Xi_j\right)\mathbf{x}_j b_j + \mathbf{e}_{q_k}^{\mathsf{T}}\mathbf{n}.\end{aligned} \tag{25}$$

AR versus TR. As well-known [33, 43], TR usually increases the kurtosis of the interference at the output of Rake receivers. This follows from the fact that the effective channel impulse response formed by the combination of prefilter and multipath channel has a peaked behavior, whereas without TR the behavior is nonpeaked. While in the single user case the two schemes are equivalent, this equivalence does not hold in the multiuser case. The impact of estimation errors will be investigated in Sections 3 and 4.

2.4. Channel Estimation and Data Transmission. For both AR and TR, the channel impulse response estimation requires cooperation between the transmitter and in the receiver. Actual transmission of the set of information-bearing symbols requires, therefore, additional symbols to be sent either in a preamble or in a postamble of the block [44]. Note that in the scenario considered in this work precoding of UT_k does not depend on channels experienced by users $j \neq k$, and thus feedback from the BS to each UT is not required (see [42] for a thorough discussion).

Assuming Time-Division Duplexing (TDD) is adopted, transmission can follow the scheme shown in Figure 3, summarizing the organization of the different links (downlink, i.e., broadcast, versus uplinks) over time, where durations of data, preamble, and postamble are indicated in terms of number of chips (N_t^{DL}, N_t^{UL}, N_{d}, N_g^{UL}). The information exchange between the BS and each UT consists in four phases:

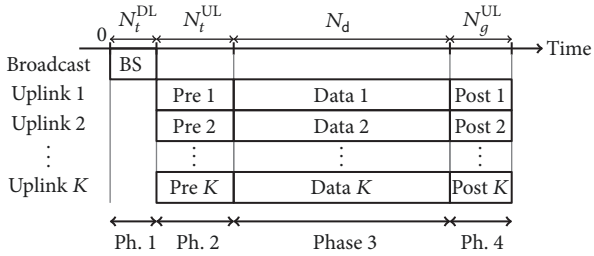

Figure 3: Channel estimation and data transmission scheme.

(1) *Phase 1, Downlink Channel Training*: the BS broadcasts a training sequence of length $N_t^{DL}\dot{\imath}$ samples (corresponding to $N_t^{DL}\dot{\imath}/\mathsf{W}$ seconds) that is received by each UT starting at time 0. Each multipath channel spreads the sequence for $L\dot{\imath}$ samples; hence each UT listens from time 0 to time $N_t^{DL}\dot{\imath} + L\dot{\imath}$ samples. This training sequence may be also used for network synchronization at symbol level.

(2) *Phase 2, Uplink Channel Training*: each UT transmits its own training sequence of length $N_t^{UL}\dot{\imath}$ samples to the BS (preamble). By reciprocity, channels spread these sequences for $L\dot{\imath}$ samples; therefore each UT remains idle for $L\dot{\imath}$ samples.

(3) *Phase 3, Data Transmission*: each UT transmits a sequence of information-bearing symbols for $N_d\dot{\imath} = nN\dot{\imath}$ samples.

(4) *Phase 4, Idle*: each UT transmits a sequence of null symbols of duration $L\dot{\imath}$ samples denoted with 0 (postamble).

During the downlink training, the BS broadcasts its training sequence to the UTs. With reference to model of Section 2, and in particular to (11) and impulsiveness index $\dot{\imath}$, the received signal at UT_k is

$$\mathbf{y}_k^{DL} = \mathbf{C}_k \boldsymbol{v}^{DL} + \mathbf{n}_k, \quad \boldsymbol{v}^{DL} = \boldsymbol{\phi}^{DL} \otimes \mathbf{e}_1^{\dot{\imath}}, \tag{26}$$

where $\mathbf{y}_k^{DL}$ is $(N_t^{DL}\dot{\imath} + L\dot{\imath}) \times 1$ vector of received samples, $\mathbf{C}_k$ is $(N_t^{DL}\dot{\imath} + L\dot{\imath}) \times N_t^{DL}\dot{\imath}$ Toeplitz channel matrix, $\boldsymbol{\phi}^{DL}$ is $N_t^{DL} \times 1$ training sequence with energy $\|\boldsymbol{\phi}\|^2$, $\boldsymbol{v}^{DL}$ is $N_t^{DL}\dot{\imath} \times 1$ training sequence accounting for impulsiveness with energy $\|\mathbf{v}\|^2 = \|\boldsymbol{\phi}\|^2$, and $\mathbf{n}_k$ is $(N_t^{DL}\dot{\imath} + L\dot{\imath}) \times 1$ white Gaussian noise vector.

Equation (26) can be rewritten as follows:

$$\mathbf{y}_k^{DL} = \boldsymbol{\Upsilon}^{DL} \mathbf{c}_k + \mathbf{n}_k, \tag{27}$$

where now $\boldsymbol{\Upsilon}^{DL}$ is a $(N_t^{DL}\dot{\imath} + L\dot{\imath}) \times L\dot{\imath}$ Toeplitz matrix and $\mathbf{c}_k$ is the $L\dot{\imath} \times 1$ channel vector.

In order to minimize the signal-plus-interference-to-noise ratio, UT_k may use an MMSE estimation of $\mathbf{c}_k$, where the interference is caused by multipath. However, the use of PN sequences as training sequences is very common, due to their good autocorrelation properties. In fact, PN sequences have periodic ACF of the following form [45, 46]:

$$\rho_\phi[i] = \begin{cases} \|\boldsymbol{\phi}\|^2 & \text{for } i = 0 \\ -\dfrac{\|\boldsymbol{\phi}\|^2}{N_t^{DL}} & \text{for } 0 < |i| \le N_t^{DL} - 1 \end{cases} \tag{28}$$

that is asymptotically impulse-like, as $N_t^{DL} \gg 1$.

Asymptotically then, and dropping the superscript DL to unclutter notation, $\boldsymbol{\Upsilon}^T\boldsymbol{\Upsilon} \approx \|\boldsymbol{\phi}\|^2\mathbf{I} = \|\boldsymbol{v}\|^2\mathbf{I}$, and MMSE reduces to a matched filter, and estimation is as follows:

$$\mathbf{z}_k \approx \boldsymbol{\Upsilon}^T\boldsymbol{\Upsilon}\mathbf{c}_k + \boldsymbol{\Upsilon}^T\mathbf{n}_k = \|\boldsymbol{v}\|^2 \mathbf{c}_k + \boldsymbol{\nu}_k, \quad \boldsymbol{\nu}_k \sim \mathcal{N}\left(\mathbf{0}, \sigma_n^2 \|\boldsymbol{v}\|^2 \mathbf{I}\right). \tag{29}$$

Dividing by $\|\boldsymbol{v}\|^2$ the previous expression yields the following:

$$\widehat{\mathbf{c}}_k \triangleq \frac{1}{\|\boldsymbol{v}\|^2}\mathbf{z}_k \approx \mathbf{c}_k + \frac{1}{\|\boldsymbol{v}\|}\boldsymbol{\nu}_k = \mathbf{c}_k + \boldsymbol{\nu}_k', \tag{30}$$

where $\boldsymbol{\nu}_k' \sim \mathcal{N}(\mathbf{0}, (\sigma_N^2/\|\boldsymbol{v}\|^2)\mathbf{I})$. Note that, as well-known (e.g., [47]), the estimation can be made as accurately as desired by increasing $\|\boldsymbol{v}\|^2$. For antipodal sequences, say $\phi[i] \in \{-\mathsf{A}_t, \mathsf{A}_t\}$ with $\mathsf{A}_t > 0$, the energy of the training sequence is $\mathsf{A}_t^2 N_t^{DL}$; therefore, $\|\boldsymbol{v}\|^2$ can be increased either by increasing power spent on training, that is, by increasing A_t, or by increasing time spent for training, that is, by increasing N_t^{DL}, or both.

In the uplink training, the BS receives the superposition of the sequences of users each filtered by the corresponding channel, that is,

$$\mathbf{y}^{UL} = \sum_{k=1}^{K} \boldsymbol{\Upsilon}_k^{UL}\mathbf{c}_k + \mathbf{n} \equiv \boldsymbol{\Upsilon}^{UL}\mathbf{c} + \mathbf{n}, \tag{31}$$

having defined

$$\boldsymbol{\Upsilon}^{UL} \triangleq \sum_{k=1}^{K} \mathbf{e}_k^T \otimes \boldsymbol{\Upsilon}_k^{UL}, \quad \mathbf{c} \triangleq \sum_{k=1}^{K} \mathbf{e}_k \otimes \mathbf{c}_k. \tag{32}$$

As previously mentioned, the superscript UL is dropped to unclutter notation.

The goal of the BS is to linearly estimate $\mathbf{c}$ by observing $\mathbf{y}$, knowing $\boldsymbol{\Upsilon}$:

$$\mathbf{z} = \mathbf{W}^T\mathbf{y} \equiv \sum_{k=1}^{K} \mathbf{e}_k \otimes \mathbf{z}_k = \mathbf{W}^T\boldsymbol{\Upsilon}\mathbf{c} + \mathbf{W}^T\mathbf{n}, \tag{33}$$

where $\mathbf{z}$ is the $KL\dot{\imath} \times 1$ vector of channel estimations, being $\mathbf{z}_k$ the $L\dot{\imath} \times 1$ vector representing $\mathbf{c}_k$ estimate, and $\mathbf{W}^T$ is the $KL\dot{\imath} \times N_t^{UL}\dot{\imath}$ matrix representing the estimator. All common linear estimators, that is, ZF (Zero-Forcing), RZF (Regularized Zero-Forcing), MMSE (minimum mean square

error), and MF (matched filter), can be described by the following expression, parametrized by ξ and ζ:

$$\mathbf{W}^{\mathsf{T}} = \left(\xi\boldsymbol{\Upsilon}^{\mathsf{T}}\boldsymbol{\Upsilon} + \zeta\mathbf{I}\right)^{-1}\boldsymbol{\Upsilon}^{\mathsf{T}}. \tag{34}$$

Indeed, MMSE is obtained with $(\xi,\zeta) = (1,\sigma_n^2)$; ZF with $(\xi,\zeta) = (1,0)$; MF with $(\xi,\zeta) = (0,1)$; RZF with $(\xi,\zeta) = (1,z)$.

In the simple case of ZF, the form assumed by (33) is as follows:

$$\begin{aligned}\mathbf{z} &= \mathbf{c} + \left(\boldsymbol{\Upsilon}^{\mathsf{T}}\boldsymbol{\Upsilon}\right)^{-1}\boldsymbol{\Upsilon}^{\mathsf{T}}\mathbf{n} \equiv \mathbf{c} + \boldsymbol{\nu},\\ \boldsymbol{\nu} &\sim \mathcal{N}\left(\mathbf{0}, \sigma_n^2\left(\boldsymbol{\Upsilon}^{\mathsf{T}}\boldsymbol{\Upsilon}\right)^{-1}\right)\end{aligned} \tag{35}$$

and, therefore, the ℓ-th tap of the channel of generic user k is

$$z_k[\ell] = c_k[\ell] + \nu_k[\ell]. \tag{36}$$

Here, $\nu_k[\ell]$ is a correlated Gaussian random variable with variance coinciding with the $((k-1)L\dot{\imath} + \ell + 1)$-th diagonal element of $\sigma_N^2(\boldsymbol{\Upsilon}^{\mathsf{T}}\boldsymbol{\Upsilon})^{-1}$.

Assuming all UTs are transmitting the same power, i.e., $\|\boldsymbol{\upsilon}_k\|^2$ is the same for each $1 \le k \le K$, the approximation $\boldsymbol{\Upsilon}_j^{\mathsf{T}}\boldsymbol{\Upsilon}_i = \|\boldsymbol{\upsilon}\|^2\mathbf{I}\delta_{ji}$ allows assuming uncorrelated estimation errors, since $\boldsymbol{\Upsilon}^{\mathsf{T}}\boldsymbol{\Upsilon} = \|\boldsymbol{\upsilon}\|^2\mathbf{I}$, and thus

$$\begin{aligned}&\mathbf{z} = \mathbf{c} + \boldsymbol{\nu},\\ &\boldsymbol{\nu} \sim \mathcal{N}\left(\mathbf{0}, \left(\frac{\sigma_N^2}{\|\boldsymbol{\upsilon}\|^2}\right)\mathbf{I}\right),\\ &N_t^{\mathrm{UL}} \gg L.\end{aligned} \tag{37}$$

2.5. Performance Indicators. In both system structures, the statistic for inferring the transmitted symbol b_k of user k can be written in the following form:

$$z_k = a_{kk}b_k + \sum_{\substack{j=1\\ j\neq k}}^{K} a_{kj}b_j + \nu_k = a_{kk}b_k + I_k + \nu_k, \tag{38}$$

where ν_k is a r.v. representing noise, and $\{a_{kj} : j = 1,\ldots,K\}$ are r.vs. depending on multipath channels, random time-hopping codes, random delays, and estimation errors.

Two Performance Indicators Are Considered.

In the *uncoded* regime, the probability of error as defined by

$$\begin{aligned}P_e = &\frac{1}{2}\mathbb{P}\left(z_k < 0 \mid b = \sqrt{\mathscr{E}}\right)\\ &+ \frac{1}{2}\mathbb{P}\left(z_k > 0 \mid b = -\sqrt{\mathscr{E}}\right)\end{aligned} \tag{39}$$

is considered.

In the *coded* regime, mutual information with Gaussian inputs and a bank of matched-filters followed by independent decoders is considered; for the generic user k, this is given by

$$I\left(b_k; z_k\right) \text{ nats/channel use}, \tag{40}$$

where $I(b_k; z_k)$ is the mutual information between the transmitted symbol b_k and the decision variable z_k. Since a channel use corresponds to $NT_{\mathrm{c}} = N\dot{\imath}/W$ seconds, the sum-rate achieved by the set of K users is

$$R \triangleq W\frac{\beta}{\dot{\imath}}I(b;z) \text{ nats/s}, \tag{41}$$

having indicated with $I(b;z)$ the mutual information (40) for a generic user. Finally, a spectral efficiency equal to

$$\mathscr{R} \triangleq \frac{\beta}{\dot{\imath}}I(b;z) \ \text{(nats/s)/Hz} \tag{42}$$

is obtained.

3. Probability of Error

3.1. Single User. The main contribution of this subsection is to show that imperfect TR and AR achieve the same probability of error, and, therefore, that the same accuracy is needed for channel estimation at transmitter and receiver in order to achieve a given error probability.

With reference to decision variables $\hat{z}^{\mathrm{TR}}$ of (17) and $\hat{z}^{\mathrm{AR}}$ of (15), the probability of error, in both cases, is

$$\begin{aligned}P_e &= \frac{1}{2}\mathbb{P}(z < 0 \mid b = \mathsf{A}) + \frac{1}{2}\mathbb{P}(z > 0 \mid b = -\mathsf{A})\\ &= \mathbb{P}(z < 0 \mid b = \mathsf{A}),\end{aligned} \tag{43}$$

where the first equality follows from b belonging to $\{-\mathsf{A}, \mathsf{A}\}$ with equal probability, and the second equality follows from the distribution of z being an even function. For the power constraint, $\mathsf{A} = \sqrt{\mathscr{E}}$ results. Equivalence of P_e for the two cases is derived by showing that $\hat{z}^{\mathrm{TR}}$ and $\hat{z}^{\mathrm{AR}}$ have the same distribution.

To this end, rewrite the decision variable $\hat{z}^{\mathrm{AR}}$ conditioned on $b = \mathsf{A}$. Without loss of generality, and for the sake of simplicity, consider $\mathbf{x} = \mathbf{e}_1$. Then

$$\begin{aligned}\hat{z}^{\mathrm{AR}} &= \|\mathbf{c}\|^2\mathsf{A} + \mathbf{c}^{\mathsf{T}}(\mathbf{n} + \boldsymbol{\xi}\mathsf{A}) + \boldsymbol{\xi}^{\mathsf{T}}\mathbf{n}\\ &= \|\mathbf{c}\|^2\mathsf{A} + \mathbf{c}^{\mathsf{T}}\boldsymbol{\xi}\mathsf{A} + \mathbf{n}^{\mathsf{T}}(\boldsymbol{\xi} + \mathbf{c}).\end{aligned} \tag{44}$$

Similarly, the decision variable $\hat{z}^{\mathrm{TR}}$ conditioned on $b = \mathsf{A}$ is

$$\hat{z}^{\mathrm{TR}} = \mathsf{A}\mathbf{c}^{\mathsf{T}}(\mathbf{c} + \boldsymbol{\xi}) + n\|\mathbf{c} + \boldsymbol{\xi}\|, \tag{45}$$

where $n \sim \mathcal{N}(0,\sigma_N^2)$. By comparing the two expressions, $\hat{z}^{\mathrm{AR}}$ is equivalent to $\hat{z}^{\mathrm{TR}}$, the equivalence being defined as producing the same P_e, iff term $\mathbf{n}^{\mathsf{T}}(\boldsymbol{\xi} + \mathbf{c})$ in $\hat{z}^{\mathrm{AR}}$ is distributed as $n\|\mathbf{c} + \boldsymbol{\xi}\|$ in $\hat{z}^{\mathrm{TR}}$. This is, indeed, the case; by choosing an orthogonal matrix $\mathbf{Q}$ such that $\mathbf{Q}(\mathbf{c} + \boldsymbol{\xi}) = \|\mathbf{c} + \boldsymbol{\xi}\|\mathbf{e}_1$, one has

$$\begin{aligned}\mathbf{n}^{\mathsf{T}}(\mathbf{c} + \boldsymbol{\xi}) &= \mathbf{n}^{\mathsf{T}}\mathbf{Q}^{\mathsf{T}}\mathbf{Q}(\mathbf{c} + \boldsymbol{\xi}) = \mathbf{n}_1'^{\mathsf{T}}\|\mathbf{c} + \boldsymbol{\xi}\|\,\mathbf{e}_1\\ &= n_1'\|\mathbf{c} + \boldsymbol{\xi}\|,\end{aligned} \tag{46}$$

where $n_1' \sim \mathcal{N}(0,\sigma_N^2)$; hence the equivalence in terms of distributions, and, therefore, probability of error is verified.

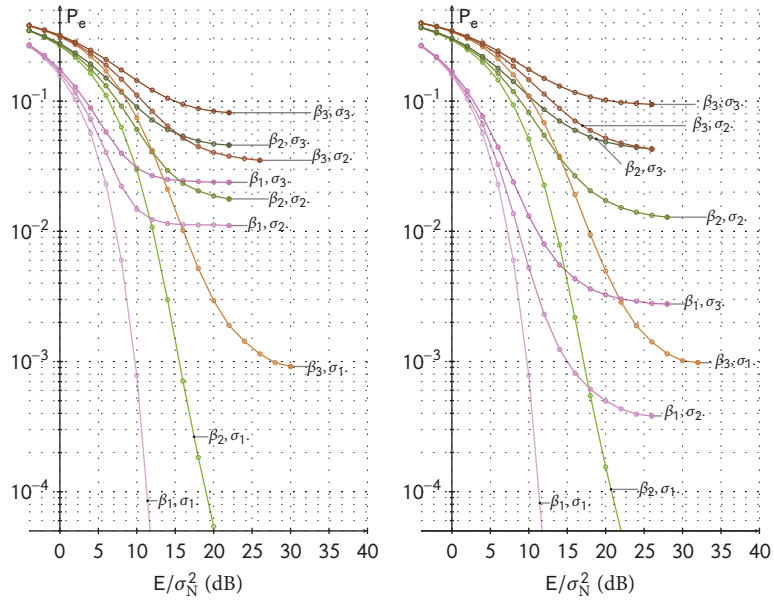

(a) *TR* (b) *AR*

FIGURE 4: Probability of error P_e versus $\mathscr{E}/\sigma_N^2$ (dB) for systems with $\dot{\iota} = 1$, $(\beta_1, \beta_2, \beta_3) = (1/200, 1/20, 1/10)$ and $(\sigma_1^2, \sigma_2^2, \sigma_3^2) = (0, 1/20, 1/10)$. Figure (a) refers to TR while (b) refers to AR.

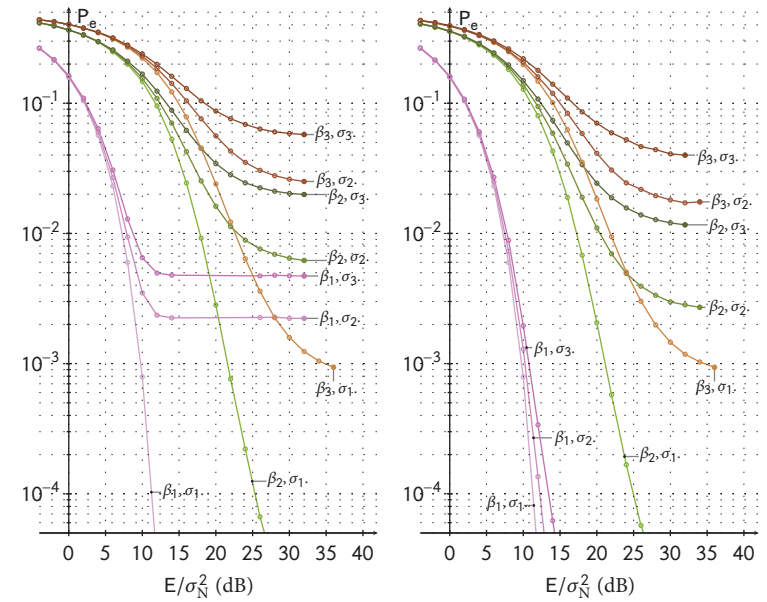

(a) *TR* (b) *AR*

FIGURE 5: Probability of error P_e versus $\mathscr{E}/\sigma_N^2$ (dB) for impulsive ($\dot{\iota} = 5$) systems with $(\beta_1, \beta_2, \beta_3) = (1/200, 1/20, 1/10)$ and $(\sigma_1^2, \sigma_2^2, \sigma_3^2) = (0, 1/20, 1/10)$. Figure (a) refers to TR while (b) refers to AR.

3.2. Multiuser. In the multiuser setting, although the expression for the probability of error remains as in (43), there are three sources of errors: thermal noise, imperfect CSI, and multiuser interference (MUI). In particular, as $\mathscr{E}/\sigma_N^2$ increases, the last two factors both lead to a probability error floor, i.e., $P_e \to P_e^{\text{floor}}(\beta, \sigma_\xi^2) > 0$ as $\mathscr{E}/\sigma_N^2 \to \infty$, being $\beta = K/N$ the load of the system.

Figures 4 and 5 show the probability of error P_e versus $\mathscr{E}/\sigma_N^2$ (dB) for systems with $\dot{\iota} = 1$ versus $\dot{\iota} = 5$, respectively, and for different values of β, with $(\beta_1, \beta_2, \beta_3) = (1/200, 1/20, 1/10)$, and σ_ξ^2, with $(\sigma_1^2, \sigma_2^2, \sigma_3^2) = (0, 1/20, 1/10)$. All results were obtained by Monte-Carlo simulations of finite-dimensional systems with $N = 200$ chips. In both figures, the left-hand side plot (Figures 4(a) and

5(a)) refers to TR, while the right-hand side plot (Figures 4(b) and 5(b)) refers to AR.

For low-SNR, i.e., $\mathscr{E} \ll \sigma_N^2$, P_e is not very sensitive to estimation errors: the performance of the systems thus mainly depends on the considered load. The impact of estimation error becomes however evident for high SNR, i.e., $\mathscr{E} \gg \sigma_N^2$, with significantly different P_e^{floor} values depending on the combination of estimation error variance σ_ξ^2 and system load (and thus MUI).

Figures 4(a) and 4(b), presenting the results for both systems with $\dot{\iota} = 1$, show that AR outperforms TR when imperfect CSI is the main cause of error (see, for example, the case (β_1, σ_2), for which the floor in the case of TR is more than an order of magnitude larger), while the opposite is true when the load is the main cause of error, with a slight advantage of TR with respect to AR for high traffic loads; see, for example, the case (β_3, σ_1) where TR guarantees a gain of about 3 dBs in terms of $\mathscr{E}/\sigma_N^2$ for a $P_e = 10^{-4}$.

Figure 5 presents results for impulsive systems, characterized by $\dot{\iota} = 5$. Focusing first on the case of perfect CSI estimation (plots with σ_1), it can be observed that, in presence of MUI, that is for medium (β_2) and high (β_3) system loads, the performance of both TR and AR is significantly worse than in the case with $\dot{\iota} = 1$. An increase of impulsiveness leads thus to a lower robustness with respect to MUI for both AR and TR schemes, although this phenomenon is arguably more evident in the TR case, since this scheme shows a slight performance advantage in the case with $\dot{\iota} = 1$, while for $\dot{\iota} = 5$ TR and AR have exactly the same performance for all system loads. When one considers the impact of CSI estimation error (plots with σ_2 and σ_3), the introduction of a more impulsive waveform has the opposite effect: both AR and TR prove to be more robust to CSI estimation errors, with lower error probability floors. The extent to which the phenomenon is visible in the two schemes is however very different: while a moderate improvement can be seen for TR, the AR scheme shows a dramatic performance increase, in particular for a low network load (β_1), where the error probability floors are not visible. The stronger positive impact of impulsiveness on the AR is a rather surprising result, which might be explained by the role of impulsiveness in the number of resolvable paths at the receiver: a shorter pulse makes in fact more paths resolvable, and TR, which allows resolving more paths than AR by approximately a factor of 2, appears to be more sensitive to estimation errors, thus reducing the advantage of increasing the impulsiveness of the system; further research is however required in order to properly explain this result.

4. Mutual Information, Sum-Rate, and Spectral Efficiency

In this section, mutual information defined in (40) is derived for AR and TR. The other merit figures defined in (41) and (42) follow directly, although all the elements for a comparison are already included in (40).

4.1. Derivation of Mutual Information. The decision variable for both the imperfect TR (cf. (25)) and AR (cf. (23)) can be cast in the following form:

$$\widehat{z}_k = \widehat{a}_{kk} b_k + \sum_{\substack{j=1 \\ j \neq k}}^{K} \widehat{a}_{kj} b_j + \widehat{\nu}_k = \widehat{a}_{kk} b_k + \widehat{S}_k + \widehat{\nu}_k, \tag{47}$$

where $\widehat{\nu}_k = n_{q_k} \sim \mathcal{N}(0, \boldsymbol{\mathcal{N}}_0/2)$.

Let us specify and give an interpretation of the terms $\widehat{a}_{ki}$, $i = 1, \ldots, K$, for both TR and AR.

TR Coupling Coefficients. For TR, the term $\widehat{a}_{kk}$ is given by

$$\begin{aligned} \widehat{a}_{kk}^{\text{TR}} &= \mathbf{e}_{q_k}^{\mathsf{T}} \mathbf{C}_k \alpha_k \left(\mathbf{T}_k + \boldsymbol{\Xi}_k\right) \mathbf{x}_k = \mathbf{c}_k^{\leftarrow \mathsf{T}} \frac{\mathbf{t}_k + \boldsymbol{\xi}_k}{\left\|\mathbf{t}_k + \boldsymbol{\xi}_k\right\|} \\ &= \mathbf{c}_k^{\mathsf{T}} \frac{\mathbf{c}_k + \boldsymbol{\xi}_k^{\leftarrow}}{\left\|\mathbf{c}_k + \boldsymbol{\xi}_k^{\leftarrow}\right\|}, \end{aligned} \tag{48}$$

where $\mathbf{v}^{\leftarrow} \in \mathbb{R}^n$ denotes a vector with same components of vector $\mathbf{v}$ in reversed order, i.e., $[\mathbf{v}^{\leftarrow}]_i = \mathbf{v}_{n-i+1}$, $1 \leq i \leq n$. The term $\widehat{a}_{kj}$, $j \neq k$, is

$$\begin{aligned} \widehat{a}_{kj}^{\text{TR}} &= \mathbf{e}_{q_k}^{\mathsf{T}} \alpha_j \mathbf{C}_j \left(\mathbf{T}_j + \boldsymbol{\Xi}_j\right) \mathbf{x}_j \\ &= \mathbf{e}_{q_k}^{\mathsf{T}} \frac{1}{\left\|\mathbf{t}_j + \boldsymbol{\xi}_j\right\|} \mathbf{C}_j \left(\mathbf{t}_j' + \boldsymbol{\xi}_j'\right) \\ &= \mathbf{e}_{q_k}^{\mathsf{T}} \frac{1}{\left\|\mathbf{t}_j + \boldsymbol{\xi}_j\right\|} \left(\boldsymbol{\gamma}_j' + \boldsymbol{\zeta}_j'\right), \end{aligned} \tag{49}$$

where $\boldsymbol{\gamma}_i' = [\mathbf{0}_{j_{\mathbf{x}_i} \times 1}^{\mathsf{T}}, \boldsymbol{\gamma}_i^{\mathsf{T}}, \mathbf{0}_{(N\dot{\iota} - j_{\mathbf{x}_i}) \times 1}^{\mathsf{T}}]^{\mathsf{T}}$ being $\boldsymbol{\gamma}_j$ the $(2(L+1)\dot{\iota} - 1) \times 1$ autocorrelation sequence of $(c_j[\ell])_{\ell=0}^{L\dot{\iota}}$, and, similarly, $\boldsymbol{\zeta}_i' = [\mathbf{0}_{j_{\mathbf{x}_i} \times 1}^{\mathsf{T}}, \boldsymbol{\zeta}_i^{\mathsf{T}}, \mathbf{0}_{(N\dot{\iota} - j_{\mathbf{x}_i}) \times 1}^{\mathsf{T}}]^{\mathsf{T}}$ with $\boldsymbol{\zeta}_i$ a Gaussian random vector with non-identity correlation.

In order to provide an interpretation of the above expressions, it is useful to start with the case of no estimation error. In general, the decision variable at the output of the matched filter of user k is given by the q_k-th sample of the sum of both intended and interference signals, plus noise. In the special case of no estimation errors, $a_{kk} = \|\mathbf{c}_k\|$ is the square-root energy of channel k, i.e., the maximum tap of the effective channel, while a_{kj} is either equal to zero if the effective channel of user j, that occupies $2(L+1)\dot{\iota} - 1$ out of $N\dot{\iota}$ degrees of freedom in a symbol period, is not present at delay q_k, or to a random resolved path of the effective channel of user j, the randomness owing to random hopping and asynchronism. In presence of estimation errors, $\widehat{a}_{kk}$ is smaller than, although in general in the neighbourhood of, the square-root energy of channel k due to the mismatch between $\widehat{\mathbf{h}}_k$ and $\mathbf{h}_k$, and $\widehat{a}_{kj}$ is either equal to zero if the *perturbed* effective channel of user j, that occupies $2(L+1)\dot{\iota} - 1$ out of $N\dot{\iota}$ degrees of freedom in a symbol period, is not present at delay q_k, or equal to a random path of the *perturbed* effective channel of user j, the perturbation owing to the imperfect channel estimation of user j.

AR Coupling Coefficients. For AR, the set of coupling coefficients $\{\widehat{a}_{ki}\}_{i=1}^{K}$ are

$$\widehat{a}_{kk}^{\mathrm{AR}} = \frac{\widehat{\mathbf{h}}_k^{\mathsf{T}}}{\left\|\widehat{\mathbf{h}}_k\right\|}\mathbf{h}_k = \left\|\mathbf{c}_k\right\|^2 + \boldsymbol{\xi}_k^{\mathsf{T}}\mathbf{c}_k, \tag{50}$$

$$\widehat{a}_{kj}^{\mathrm{AR}} = \frac{\widehat{\mathbf{h}}_k^{\mathsf{T}}}{\left\|\widehat{\mathbf{h}}_k\right\|}\mathbf{h}_j, \quad j \neq k \tag{51}$$

where $\widehat{\mathbf{h}}_k = \mathbf{h}_k + \boldsymbol{\chi}_k$, $\mathbf{h}_k = \mathbf{C}_k\mathbf{x}_k$, and $\boldsymbol{\chi}_k = \boldsymbol{\Xi}_k\mathbf{x}_k$. We can think of $\widehat{\mathbf{h}}_k/\|\widehat{\mathbf{h}}_k\|$ as the perturbed direction along which the received signal is projected in order to decode user k; $\widehat{a}_{kk}^{\mathrm{AR}}$ represents, therefore, the "mismatch" between the perturbed and unperturbed channels of user k; $\widehat{a}_{kj}^{\mathrm{AR}}$ represents the coupling between user k, that is perturbed, and another user j. As in the TR case, a channel impulse response occupies a fraction, that is approximately equal to $(L+1)/N$, of the available degrees of freedom in a symbol period; opposite of the TR case, where the perturbation affects user j in $\widehat{a}_{kj}^{\mathrm{TR}}$, user k is perturbed in the AR case (through $\widehat{\mathbf{h}}_k$) and user j appears with the true channel impulse response $\mathbf{h}_j$.

Derivation. Being each term in the r.h.s. of (47) independent of the other terms, mutual information $I(z_k; b_k)$ can be derived once the distributions of $\widehat{a}_{kk}$ and $\widehat{S}_k$ are known. The former depends on both the random channel impulse response and estimation errors of user k, and the latter on the random channel impulse responses and estimation errors, and the random delays with respect to user k. Hence, the final form assumed by $I(z_k; b_k)$ strongly depends on the channel model; however, in the following, the effect of the time-hopping and random asynchronism will be enucleated, without entering in the computation of a mutual information when a particular channel model is adopted; this last task was addressed by simulations, where Channel Model 1 (CM1) specified in the IEEE 802.15.3a standard [48], that is valid for bandwidths up to several gigahertz, was selected. Details on the settings and results of these simulations are provided in Section 4.2.

In the case of TR, since the effective channel of user j occupies a fraction $f = (2(L+1)\imath - 1)/(N\imath)$, and user k, due to the assumptions on independence and uniformity of hopping codes and asynchronism, selects uniformly at random one of the $N\imath$ samples available per symbol period, then a_{kj}, $j \neq k$, is equal to zero with probability $1 - f$, and is distributed as the generic path of the effective channel $\mathbf{h}_j$ with probability f, that is

$$P_{a_{kj}^{\mathrm{TR}}} = (1 - f)\,\delta_0 + fP^{\mathrm{TR}}, \tag{52}$$

where P^{TR} indicates the distribution of the generic path of the effective channel of user j (that is independent of j). In presence of estimation errors, the above argument holds, that is, $\widehat{a}_{kj}$, $j \neq k$, is equal to zero with probability $1 - f$, and is distributed as the generic path of the *perturbed* effective channel $\widehat{\mathbf{h}}_j$ with probability f:

$$P_{\widehat{a}_{kj}^{\mathrm{TR}}} = (1 - f)\,\delta_0 + f\widehat{P}^{\mathrm{TR}}, \tag{53}$$

where $\widehat{P}^{\mathrm{TR}}$ indicates the distribution of the generic path of the *perturbed* effective channel of user j (that is independent of j).

In the case of AR, let us start by finding the distribution of a_{kj}, $j \neq k$, i.e., the coupling coefficient between two users in absence of estimation error. Each channel spans a subspace of dimension $(L+1)\imath$ in a space with $(N+L+1)\imath - 1$ dimensions (the number of degrees of freedom in a symbol period is $N\imath$; in the large system limit, as $N \gg L$, the difference between $(N+L+1)\imath - 1$ and $N\imath$ due to the convolution is negligible.); in other words, just $(L+1)\imath$ entries of $\mathbf{h}_i$ are nonzero. From the hypotheses of independence and uniformity of delays due to asynchronism between users and time-hopping codes, there exists a probability f such that the inner product $\mathbf{h}_k^{\mathsf{T}}\mathbf{h}_j$ is nonzero, and the remaining probability $1 - f$ that the inner product is zero. We may think of the "nonzero event" as the partial overlapping between two channels. As $N \gg L$, $f \approx (2(L+1)\imath - 1)/(N\imath)$ results, where the assumption $N \gg L$ allows neglecting border effects. Indicating with P^{AR} the distribution of a_{kj}^{AR} conditioned on the nonzero event, one has the following:

$$P_{a_{kj}^{\mathrm{AR}}} = (1 - f)\,\delta_0 + fP^{\mathrm{AR}}. \tag{54}$$

In presence of estimation errors, the above discussion remains valid, since an error $\boldsymbol{\chi}_k$ changes, in general, the direction of vector $\widehat{\mathbf{h}}_k$ with respect to $\mathbf{h}_k$, i.e., $\widehat{\mathbf{h}}_k$ and $\mathbf{h}_k$, is, in general, not colinear, but it does not change the subspace spanned by the two channels, i.e., the subspace spanned by the true channel is equal to the subspace spanned by the perturbed channel. Indicating with $\widehat{P}^{\mathrm{AR}}$ the distribution of $\widehat{a}_{kj}^{\mathrm{AR}}$ conditioned on the nonzero event, one has the following:

$$P_{\widehat{a}_{kj}^{\mathrm{AR}}} = (1 - f)\,\delta_0 + f\widehat{P}^{\mathrm{AR}}. \tag{55}$$

$\widehat{P}^{\mathrm{AR}}$ reduces to P^{AR} when the estimation error is nil.

In terms of c.fs., (55) and (53) become the following:

$$\varphi_{\widehat{a}_{kj}}(u) = \mathbb{E}\left[e^{ju\alpha}\right] = 1 - f\left(1 - \widehat{\varphi}(u)\right), \tag{56}$$

where

$$\widehat{\varphi}(u) = \int_{\mathbb{R}} d\alpha e^{j\alpha u}\widehat{P}(\alpha), \tag{57}$$

being $\widehat{P}$ equal to either $\widehat{P}^{\mathrm{AR}}$ or $\widehat{P}^{\mathrm{TR}}$ in (55) and (53), respectively. In general, given two independent r.vs. X and Y and their product $Z = XY$, $\varphi_Z(u) = \mathbb{E}[\varphi_Y(uX)] = \mathbb{E}[\varphi_X(uY)]$ results; therefore, the r.v. $\widehat{a}_{kj}b_j$ has c.f.:

$$\begin{aligned}\varphi_{\widehat{a}_{kj}b_j}(u) &= \mathbb{E}\left[\varphi_{\widehat{a}_{kj}}\left(b_j u\right)\right] = 1 - f\left(1 - \mathbb{E}\left[\widehat{\varphi}\left(b_j u\right)\right]\right) \\ &= 1 - f\left(1 - \overline{\varphi}(u)\right),\end{aligned} \tag{58}$$

where the expectation is taken with respect to $b_j \sim \mathcal{N}(0, \mathscr{E})$, and $\overline{\varphi}(u)$ is independent of j. Since $\{\widehat{a}_{kj}b_j\}$ with $j \in \{1, \ldots, K\}\backslash k$ are independent, $\widehat{S}_k$ has c.f.:

$$\varphi_{\widehat{S}_k}(u) = \left\{1 - \frac{2(L+1)\imath - 1}{N\imath}\left(1 - \overline{\varphi}(u)\right)\right\}^{K-1}, \tag{59}$$

that, in the large system limit, where $K \to \infty$, $N \to \infty$, $K/N \to \beta$, converges to

$$\varphi_{\widehat{S}_k}(u) = e^{-\beta_{\text{eff}}[1-\overline{\varphi}(u)]} = \sum_{r\geq 0} \frac{\beta_{\text{eff}}^r}{r!} e^{-\beta_{\text{eff}}} \left[\overline{\varphi}(u)\right]^r, \tag{60}$$

where $\beta_{\text{eff}} = \beta(2(L+1)\dot{\iota} - 1)/\dot{\iota}$ is the effective load; without multipath ($L = 1$) and one pulse per chip ($\dot{\iota} = 1$), β_{eff} reduces to the usual load β as given by K/N. The interference-plus-noise variable has thus c.f. given by the following:

$$\varphi_{\widehat{S}_k+\widehat{\nu}_k}(u) = \varphi_{\widehat{S}_k}(u)\,\varphi_{\widehat{\nu}_k}(u) = e^{-\beta_{\text{eff}}[1-\overline{\varphi}(u)]-(\sigma_N^2/2)u^2}. \tag{61}$$

Knowing the distribution of z_k conditioned on b_k, or equivalently its c.f., mutual information $I(z_k; b_k) = h(z_k) - h(z_k \mid b_k)$ follows directly. Hence, the c.f. of z_k given b_k is the following:

$$\varphi_{\widehat{z}_k|b_k}(u) = \varphi_{\widehat{S}_k+\widehat{\nu}_k}(u)\,\varphi_{\widehat{a}_{kk}}(b_k u); \tag{62}$$

hence, the c.f. of $\widehat{z}_k$ is as follows:

$$\varphi_{\widehat{z}_k}(u) = \mathbb{E}\left[\varphi_{\widehat{z}_k|b_k}(u)\right] = \varphi_{\widehat{S}_k+\widehat{\nu}_k}(u)\,\mathbb{E}\left[\varphi_{\widehat{a}_{kk}}(b_k u)\right], \tag{63}$$

where the expectation is over $b_k \sim \mathcal{N}(0, \mathscr{E})$. Explicitly, one has the following:

$$h(\widehat{z}_k) = \int_{\mathbb{R}} -P_{\widehat{z}_k}(z) \ln P_{\widehat{z}_k}(z)\, dz, \tag{64}$$

where

$$P_{\widehat{z}_k}(z) = \frac{1}{2\pi} \int_{\mathbb{R}} du e^{-juz} \varphi_{\widehat{z}_k}(u), \tag{65}$$

and

$$\begin{aligned} h(\widehat{z}_k \mid b_k) &= \int_{\mathbb{R}} \Phi_{0,\mathscr{E}}(b)\, h\left(\widehat{a}_{kk} b + \widehat{S}_k + \widehat{\nu}_k\right) \\ &= \int_{\mathbb{R}} \Phi_{0,\mathscr{E}}(b) \int_{\mathbb{R}} -P_{\widehat{z}_k|b_k=b}(z) \ln P_{\widehat{z}_k|b_k=b}(z)\, dz, \end{aligned} \tag{66}$$

where $\Phi_{0,\mathscr{E}}$ denotes a Gaussian distribution with zero mean and variance $\mathscr{E}$, and

$$P_{\widehat{z}_k|b_k=b}(z) = \frac{1}{2\pi} \int_{\mathbb{R}} du e^{-juz} \varphi_{\widehat{z}_k|b_k=b}(u). \tag{67}$$

The above derivation allows one to find $I(\widehat{z}_k; \widehat{b}_k) = h(\widehat{z}_k) - h(\widehat{z}_k \mid b_k)$ as a function of the distribution $\widehat{P}$ of $\widehat{a}_{kj}$, $j \neq k$, and the distribution $P_{\widehat{a}_{kk}}$ accounting for the loss of correlation incurred by the user to be decoded because of the estimation error. Both $\widehat{P}$ and $P_{\widehat{a}_{kk}}$ account for the channel model and the estimation error, in particular its variance.

As baseline comparison, we also provide the following lower bound $\underline{I}(\widehat{z}_k; b_k)$ for $I(\widehat{z}_k; b_k)$, that is achieved when the interference is Gaussian:

$$\begin{aligned} I(\widehat{z}_k; b_k) &\geq \underline{I}(\widehat{z}_k; b_k) \\ &= \mathbb{E}\left[\frac{1}{2} \ln\left(1 + \frac{\mathscr{E}\widehat{a}_{kk}^2}{\text{var}\left[\widehat{S}_k\right] + \text{var}\left[\widehat{\nu}_k\right]}\right)\right], \end{aligned} \tag{68}$$

where the expectation is over $\widehat{a}_{kk}$. The corresponding spectral efficiency lower bound is $\underline{\mathscr{R}} = (\beta/\dot{\iota})\underline{I}(\widehat{z}_k; b_k)$ (cf. (42)).

Results are shown on Figure 6, where $\mathscr{R}$ (solid curve) and $\underline{\mathscr{R}}$ (dashed curve) are presented as a function of $\mathscr{E}/\sigma_N^2$, for different values of β and σ_ξ^2. The receiver structure shows a mutual information floor at high SNR. By comparing Figures 6(a) and 6(b), one observes that $\mathscr{R}$ increases sublinearly as β increases, while by comparing Figures 6(a) and 6(c), or Figures 6(b) and 6(d), a reduction in spectral efficiency due to the presence of an estimation error is observed. $\mathscr{R}$ scales with $\dot{\iota}$ as shown on Figures 6(e) and 6(f).

For all results presented in Figure 6, AR outperforms TR, again indicating that, under the assumptions considered in this work, performance of TR is significantly degraded by channel estimation errors. It is interesting to note, however, that the gap $\mathscr{R} - \underline{\mathscr{R}}$ can be interpreted as a measure of the non-Gaussianity of $\widehat{z}_k$ and $\widehat{z}_k \mid b_k$, and is indeed higher in the TR case with respect to the AR case, because of the different distribution of the interference term. A detailed discussion on the characteristics of interference is provided in the next subsection.

4.2. Impact of Channel Model and Interference Distribution. As previously said, the distributions of the channel paths and in turn of the coupling coefficients used in (52)-(55) depend on the channel model and were obtained by simulation. All simulations were carried out for a system with fixed chip duration $T_c = 1$ ns and bandwidth $\mathsf{W} = \dot{\iota}/T_c$. Power control was assumed; in particular, $\|\mathbf{c}_k\|^2 = 1$ for all users, $k = 1, \ldots, K$. The delay spread of each channel impulse response was fixed at a value $T_d = 50$ ns that includes most of the energy of typical CM1 channels. For a given bandwidth W, the length of the channel expressed in number of samples per channel is $T_d\mathsf{W}$; i.e., $\mathbf{c}_k$ is a $(\lfloor T_d\mathsf{W} \rfloor + 1) \times 1$ vector.

Figure 7 shows the distributions P^{TR}, $\widehat{P}^{\text{TR}}$, P^{AR}, and $\widehat{P}^{\text{AR}}$ in (52), (53), (54), and (55), respectively, and the distribution $P_{\widehat{a}}$ of the term $\widehat{a}_{kk}$.

Figure 7(a) versus Figure 7(b), in particular, shows the distributions of the coupling coefficient a_{kj}, $j \neq k$, in case of no estimation errors, for AR and TR, respectively. As may be expected, the variance of the latter is larger than the variance of the former, as follows from the property of TR to increase the total energy of the effective channel; in the specific case, one has $\text{var}[a_{kj}^{\text{AR}}] \approx 0.0099$, while $\text{var}[a_{kj}^{\text{TR}}] \approx 0.0173$. In Figure 7(b) the presence of a strong interference ($a_{kj}^{\text{TR}} = 1$) is highlighted, not present in the AR case; this is coherent with the fact that, in the TR case, there is, indeed, among the $2(L+1)\dot{\iota} - 1$ paths of the effective channel, one path with amplitude equal to the square-root energy of the channel, $\|\mathbf{c}_k\| = 1$, that is, therefore, selected with probability $1/(2(L+1)\dot{\iota} - 1)$. P^{TR} is also more leptokurtic than P^{AR}, showing a kurtosis approximately equal to 34 for TR versus 12 for the AR variable. Figure 7(c) versus Figure 7(d) shows the distributions of the coupling coefficient $\widehat{a}_{kj}$, $j \neq k$, in case of estimation error with per sample variance $\sigma_\xi^2 = 0.01$, for AR and TR, respectively. Even in presence of CSI estimation error, both variance and kurtosis of TR are larger than those

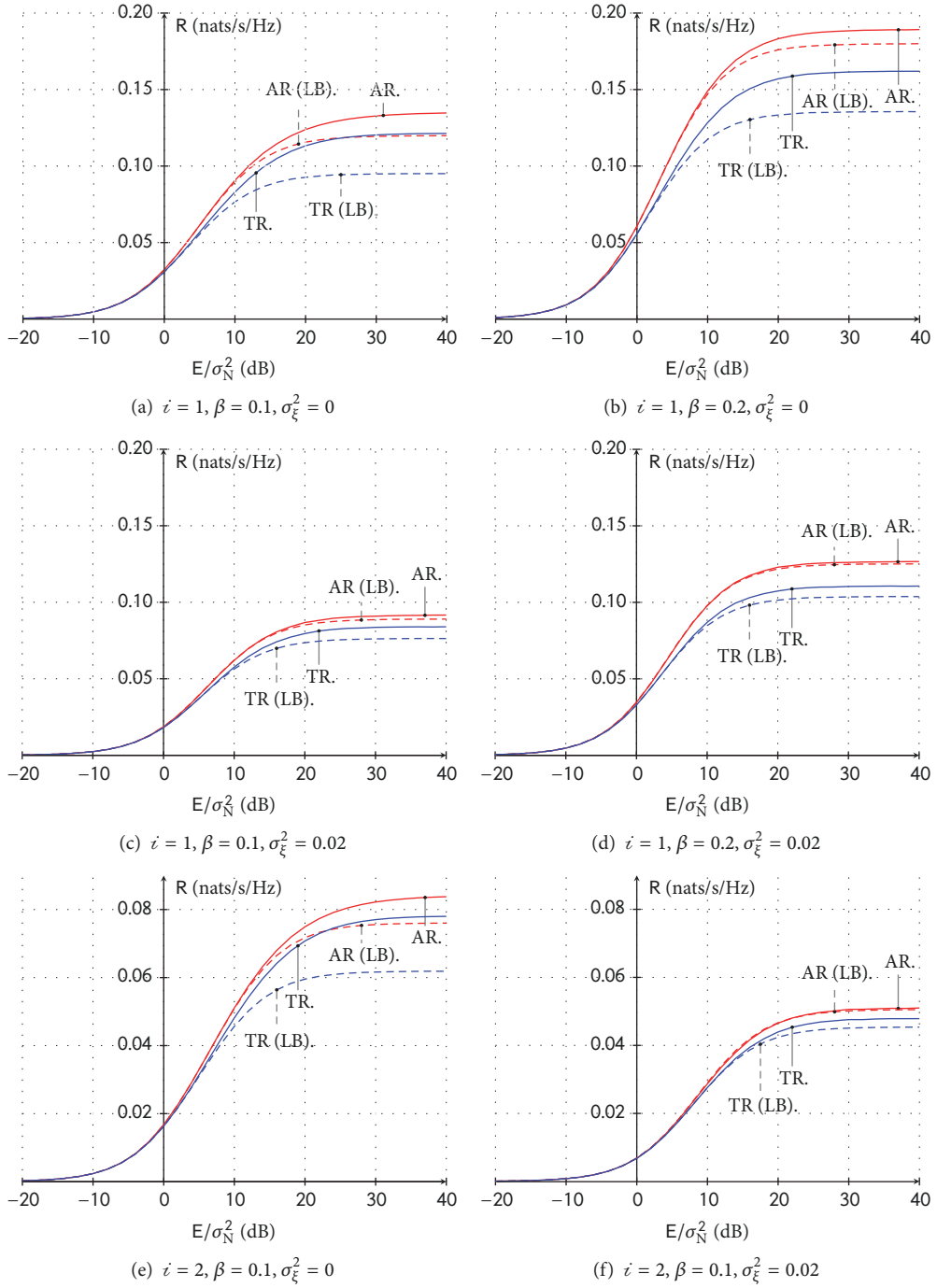

(a) $\imath = 1, \beta = 0.1, \sigma_\xi^2 = 0$ (b) $\imath = 1, \beta = 0.2, \sigma_\xi^2 = 0$

(c) $\imath = 1, \beta = 0.1, \sigma_\xi^2 = 0.02$ (d) $\imath = 1, \beta = 0.2, \sigma_\xi^2 = 0.02$

(e) $\imath = 2, \beta = 0.1, \sigma_\xi^2 = 0$ (f) $\imath = 2, \beta = 0.1, \sigma_\xi^2 = 0.02$

FIGURE 6: Spectral efficiency $\mathscr{R}$ (solid curve) and lower bound assuming Gaussian interference (dashed curve) versus $\mathsf{SNR} = \mathscr{E}/\sigma_N^2$ (dB) for different values of load β and error variance σ_ξ^2. Impulsiveness index is fixed to $\imath = 1$ in Figs. from (a) to (d) and to $\imath = 2$ in Figs. (e) and (f).

of AR; in particular, one has $\mathrm{var}[a_{kj}^{\mathrm{AR}}] \approx 0.0099$ versus $\mathrm{var}[a_{kj}^{\mathrm{TR}}] \approx 0.0149$, and $\mathrm{kurt}[a_{kj}^{\mathrm{AR}}] \approx 6.9$ versus $\mathrm{kurt}[a_{kj}^{\mathrm{TR}}] \approx 21.7$. Figure 7(e) shows the distribution of the term $\widehat{a}_{kk}$, that is the same for both TR and AR, and is represented for $\sigma_\xi^2 = 0.01$.

Figure 8 shows distributions $\overline{P}$, $P_{\widehat{S}}$, $P_{\widehat{\nu}}$, and $P_{\widehat{S}+\widehat{\nu}}$, that correspond to c.fs. $\overline{\varphi}$, $\varphi_{\widehat{S}}$, $\varphi_{\widehat{\nu}}$, and $\varphi_{\widehat{S}+\widehat{\nu}}$ defined above, for different values of σ_ξ^2 and $\mathsf{SNR} = \mathscr{E}/\sigma_N^2$, and fixed value of load $\beta = 0.1$. Figures 8(a) and 8(b) show a noise-limited scenario, where $\mathsf{SNR} = 0$ dB, without and with estimation errors, respectively: simulations show that the interference-plus-noise variable is not significantly affected by estimation errors (cf. $P_{S+\nu}$ and $P_{\widehat{S}+\widehat{\nu}}$ curves), although P_S, as well as $\overline{P}$, becomes less leptokurtic in presence of estimation errors. Figures 8(c) and 8(d) show an interference-limited scenario, where $\mathsf{SNR} = 20$ dB: in this case P_S is far from Gaussian, and

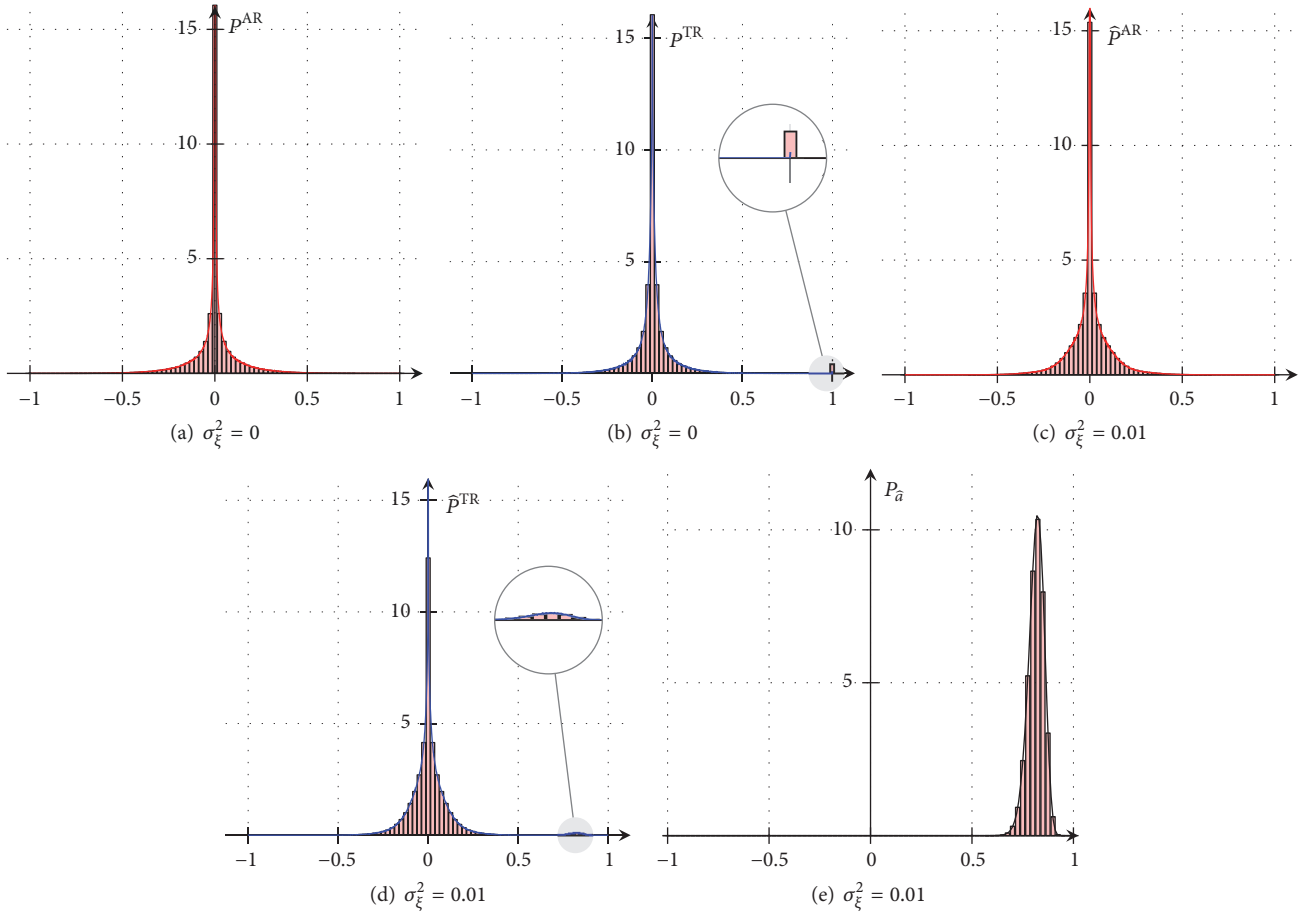

FIGURE 7: PDFs $\widehat{P}$ and $P_{\widehat{a}}$ of the variables $\widehat{a}_{kj}$, $j \neq k$, and $\widehat{a}_{kk}$, respectively. Distributions do not depend on the particular user k. Figs. (a) and (b) correspond to a variable $\widehat{a}_{kj}$, $j \neq k$, in systems without estimation errors; Figs. (c) and (d) correspond to a variable $\widehat{a}_{kj}$, $j \neq k$, in systems with estimation errors with variance $\sigma_\xi^2 = 0.01$; Fig. (e) corresponds to a variable $\widehat{a}_{kk}$ in systems with the same error variance.

so is the interference-plus-noise PDF $P_{S+\nu}$; the effect of the estimation error is to decrease the kurtosis of P_S, and so that of $P_{S+\nu}$.

As a summary, results show that TR leads to a more leptokurtic interference distribution, even in presence of estimation errors. It was however shown in the past that the non-Gaussianity of interference can be taken advantage of by an adapted receiver structure [43, 49]: it can be thus expected that TR could benefit more than AR in case a different receiver structure taking into account the non-Gaussianity of interference were to be adopted and in turn reduce or compensate the gap in performance observed with the receiver considered in this work, not adapted to the MUI distribution. The performance improvement would heavily depend on the specific channel characteristics, suggesting that the choice between AR and TR should be performed taking into account the characteristics of the signal and of the propagation channel.

5. Conclusions and Future Investigations

In this paper the problem of characterizing system performance for single-antenna systems using TR in the case of imperfect channel estimation was addressed. The reference network model included one BS and several UTs, and the uplink communication channel was considered in the investigation, representing a scenario where devices with similar characteristics play different role in a D2D network. TR was compared against a reference configuration with no prefiltering and AR at the receiver.

The effect of imperfect channel estimation on both transceiver configurations was analyzed, also taking into account the degree of impulsiveness of the transmission waveform. Channel estimation error was modeled as an additive Gaussian noise based on the output of a training phase that was used to tune transmitter and receiver structures. The comparison was performed for both the single user channel and the multiuser channel with power control. Modeling of the channels was obtained based on the 802.15.3a CM1 model. The two communication schemes, TR and AR, were compared based on two different performance indicators: probability of error and mutual information as a function of signal-to-noise ratio.

Results highlighted that, for the single user channel, probability of error for TR and AR coincided, while for the multiuser channel, the two schemes had similar performance

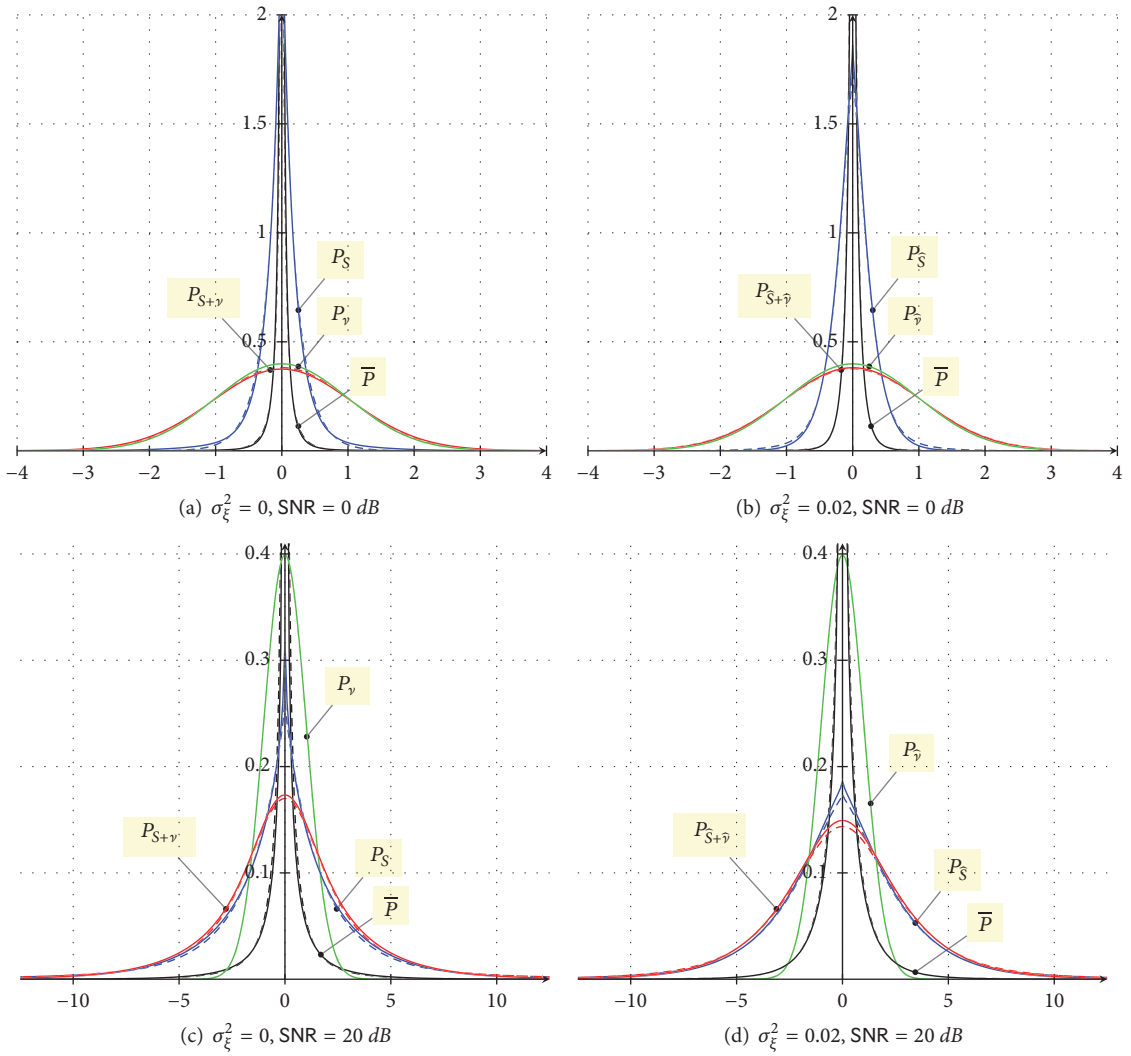

FIGURE 8: PDF $\overline{P}$ of interfering terms $\widehat{a}_{kj}b_j$, $j \neq k$, given $\widehat{a}_{kj} \neq 0$, $P_{\widehat{\nu}}$ of the noise variable $\widehat{\nu}_k$, $P_{\widehat{S}}$ of interference $\widehat{S}_k$, and $P_{\widehat{S}+\widehat{\nu}}$ of interference-plus-noise $\widehat{S}_k + \widehat{\nu}_k$. Error variance σ_ξ^2 and SNR $= \mathscr{E}/\sigma_N^2$ are specified below each subfigure. The noise variance σ_N^2 is normalized to 1. The load β of the network is fixed and equal to $\beta = 0.1$. Solid versus dashed curves refer to TR versus AR, respectively.

when the load, as measured by the ratio between the number of terminals K and the number of chips N in a symbol period, $\beta = K/N$, was the main cause of error, irrespectively of the degree of impulsiveness; oppositely, AR outperformed TR when imperfect CSI was the main cause of error in impulsive systems, suggesting a higher robustness of AR to CSI estimation error, related to the different number of resolvable paths between the two schemes.

In terms of spectral efficiency, a lower bound expression was provided, and the two schemes were analyzed under different impulsiveness index $\imath$ and load β. Results expressed by spectral efficiency $\mathscr{R}$ (nats/s/Hz) as a function of signal-to-noise ratio indicated that, for low-SNR, $\mathscr{R}$ was similar for the two systems, while, for higher SNR values, AR outperformed TR. In all cases, however, TR led to a more leptokurtic MUI noise.

In summary the following observations can be drawn based on the analysis carried out in this work: (1) both AR and TR benefit from the use of a more impulsive waveform, with an increase in robustness to CSI estimation errors; (2) AR outperforms TR if a simple receiver not matched to the MUI statistics is taken into account; (3) the MUI statistics confirm however that, even in presence of CSI estimation error, TR leads to a significantly non-Gaussian MUI, that could be taken advantage of with a different receiver structure adapted to the MUI, possibly compensating the gap between TR and AR.

Future work will indeed investigate the use of different receiver structures capable of taking advantage of the pronounced non-Gaussianity of interference in the TR case but will also extend the work towards more complex receiver schemes, such as multiuser detection, to provide a fair comparison.

Data Availability

Data presented in the manuscript are available upon request by contacting the corresponding author.

Conflicts of Interest

The authors declare that there are no conflicts of interest regarding the publication of this paper.

Acknowledgments

The work of L. De Nardis and M.-G. Di Benedetto was supported by Sapienza University of Rome within research projects with Grants nos. RP11715C7EFAA443, RP11715C7CA5279D, and RM116155068578FB.

References

[1] S. A. Schelkunoff, "Some equivalence theorems of electromagnetics and their application to radiation problems," *Bell System Technical Journal*, vol. 15, no. 1, pp. 92–112, 1936.

[2] S. A. Schelkunoff, "On diffraction and radiation of electromagnetic waves," *Physical Review A: Atomic, Molecular and Optical Physics*, vol. 56, no. 4, pp. 308–316, 1939.

[3] J. A. Stratton and L. J. Chu, "Diffraction theory of electromagnetic waves," *Physical Review A: Atomic, Molecular and Optical Physics*, vol. 56, no. 1, pp. 99–107, 1939.

[4] K.-M. Chen, "A mathematical formulation of the equivalence principle," *IEEE Transactions on Microwave Theory and Techniques*, vol. 37, no. 10, pp. 1576–1581, 1989.

[5] M. Fink, "Time reversal of ultrasonic fields. I. Basic principles," *IEEE Transactions on Ultrasonics, Ferroelectrics and Frequency Control*, vol. 39, no. 5, pp. 555–566, 1992.

[6] A. Derode, P. Roux, and M. Fink, "Robust acoustic time reversal with high-order multiple scattering," *Physical Review Letters*, vol. 75, no. 23, pp. 4206–4209, 1995.

[7] M. Fink, G. Montaldo, and M. Tanter, "Time reversal acoustics," in *Proceedings of the IEEE Ultrasonics Symposium*, pp. 850–859, Montreal, Canada, 2004.

[8] M. Z. Shakir, M. Ismail, X. Wang, K. A. Qaraqe, and E. Serpedin, "From D2D to Ds2D: prolonging the battery life of mobile devices via ds2d communications," *IEEE Wireless Communications Magazine*, vol. 24, no. 4, pp. 55–63, 2017.

[9] "5G: a technology vision," http://www.huawei.com/5gwhitepaper/, 2013.

[10] R. Esmailzadeh and M. Nakagawa, "Pre-Rake diversity combination for direct sequence spread spectrum communications systems," in *Proceedings of the IEEE International Conference on Communications '93*, pp. 463–467, May 1993.

[11] R. Esmailzadeh and M. Nakagawa, "Pre-RAKE diversity combination for direct sequence spread spectrum mobile communications systems," *IEICE Transactions on Communications*, vol. E76-B, no. 8, pp. 1008–1015, 1993.

[12] Z. Tang and S. Cheng, "Interference cancellation for DS-CDMA systems over flat fading channels through pre-decorrelating," in *Proceedings of the IEEE Personal, Mobile and Radio Communications (PIMRC)*, vol. 2, pp. 435–438, The Hague, Netherlands, 1994.

[13] M. Joham, W. Utschick, and J. A. Nossek, "On the equivalence of prerake and transmit matched filter," in *Proceedings of the in 10th Aachen Symposium on Signal Theory*, pp. 313–318, September 2001.

[14] M. Joham, W. Utschick, and J. A. Nossek, "Linear transmit processing in MIMO communications systems," *IEEE Transactions on Signal Processing*, vol. 53, no. 8, part 1, pp. 2700–2712, 2005.

[15] A. N. Barreto and G. Fettweis, "Capacity increase in the downlink of spread spectrum systems through joint signal precoding," *IEEE International Conference on Communications*, vol. 4, pp. 1142–1146, 2001.

[16] B. R. Vojcic and W. M. Jang, "Transmitter precoding in synchronous multiuser communications," *IEEE Transactions on Communications*, vol. 46, no. 10, pp. 1346–1355, 1998.

[17] M. Vu and A. Paulraj, "MIMO wireless linear precoding," *IEEE Signal Processing Magazine*, vol. 24, no. 5, pp. 86–105, 2007.

[18] D. P. Palomar and Y. Jiang, "MIMO transceiver design via majorization theory," *Foundations and Trends in Communications and Information Theory*, vol. 3, no. 4-5, pp. 331–551, 2006.

[19] L. Cao and N. C. Beaulieu, "Closed-form BER results for MRC diversity with channel estimation errors in Ricean fading channels," *IEEE Transactions on Wireless Communications*, vol. 4, no. 4, pp. 1440–1447, 2005.

[20] F. J. Lopez-Martinez, E. Martos-Naya, J. F. Paris, and U. Fernandez-Plazaola, "Generalized BER analysis of QAM and its application to MRC under imperfect CSI and interference in ricean fading channels," *IEEE Transactions on Vehicular Technology*, vol. 59, no. 5, pp. 2598–2604, 2010.

[21] Y. Ma and J. Jin, "Effect of channel estimation errors on M-QAM With MRC and EGC in Nakagami fading channels," *IEEE Transactions on Vehicular Technology*, vol. 56, no. 3, pp. 1239–1250, 2007.

[22] R. Schober and D. Zhang, "Exact BER for M-QAM with MRC and imperfect channel estimation in Rician fading channels," *IEEE Transactions on Wireless Communications*, vol. 6, no. 3, pp. 926–936, 2007.

[23] T. Strohmer, M. Emami, J. Hansen, G. Papanicolaou, and A. J. Paulraj, "Application of time-reversal with MMSE equalizer to UWB communications," in *Proceedings of the GLOBECOM'04 - IEEE Global Telecommunications Conference*, pp. 3123–3127, December 2004.

[24] A. E. Akogun, R. C. Qiu, and N. Guo, "Demonstrating the leverages of time reversal in ultra-wideband communications using time domain measurements," in *Proceedings of the 51st International Instrumentation Symposium*, pp. 737–742, May 2005.

[25] H. T. Nguyen, J. B. Andersen, G. F. Pedersen, P. Kyritsi, and P. C. F. Eggers, "Time reversal in wireless communications: a measurement-based investigation," *IEEE Transactions on Wireless Communications*, vol. 5, no. 8, pp. 2242–2251, 2006.

[26] R. C. Qiu, C. Zhou, N. Guo, and J. Q. Zhang, "Time reversal with MISO for ultrawideband communications: experimental results," *IEEE Antennas and Wireless Propagation Letters*, vol. 5, no. 1, pp. 269–273, 2006.

[27] C. Zhou, N. Guo, and R. C. Qiu, "Time-reversed ultra-wideband (UWB) multiple input multiple output (MIMO) based on measured spatial channels," *IEEE Transactions on Vehicular Technology*, vol. 58, no. 6, pp. 2884–2898, 2009.

[28] N. Guo, B. M. Sadler, and R. C. Qiu, "Reduced-complexity UWB time-reversal techniques and experimental results," *IEEE Transactions on Wireless Communications*, vol. 6, no. 12, pp. 4221–4226, 2007.

[29] R. C. Qiu, J. Q. Zhang, and N. Guo, "Detection of physics-based ultra-wideband signals using generalized RAKE with multiuser detection (MUD) and time-reversal mirror," *IEEE Journal on Selected Areas in Communications*, vol. 24, no. 4 I, pp. 724–730, 2006.

[30] R. C. Qiu, "A generalized time domain multipath channel and its application in ultra-wideband (UWB) wireless optimal

receiver—Part III: system performance analysis," *IEEE Transactions on Wireless Communications*, vol. 5, no. 10, pp. 2685–2695, 2006.

[31] G. C. Ferrante, J. Fiorina, and M.-G. Di Benedetto, "Complexity reduction by combining time reversal and IR-UWB," in *Proceedings of the 2012 IEEE Wireless Communications and Networking Conference, WCNC*, pp. 28–31, April 2012.

[32] G. C. Ferrante, J. Fiorina, and M.-G. Di Benedetto, "Time reversal beamforming in MISO-UWB channels," in *Proceedings of the 2013 IEEE International Conference on Ultra-Wideband (ICUWB)*, pp. 261–266, Sydney, New South Wales, Australia, September 2013.

[33] L. De Nardis, J. Fiorina, D. Panaitopol, and M.-G. Di Benedetto, "Combining UWB with Time Reversal for improved communication and positioning," *Telecommunication Systems*, vol. 52, no. 2, pp. 1145–1158, 2013.

[34] I. H. Naqvi, P. Besnier, and G. E. Zein, "Robustness of a time-reversal ultra-wideband system in non-stationary channel environments," *IET Microwaves, Antennas & Propagation*, vol. 5, no. 4, pp. 468–475, 2011.

[35] S. Alizadeh, H. Khalegi Bizaki, and M. Okhovvat, "Effect of channel estimation error on performance of time reversal-UWB communication system and its compensation by prefilter," *IET Communications*, vol. 6, no. 12, pp. 1781–1794, 2012.

[36] D. Abbasi-Moghadam and V. T. Vakili, "Effect of channel estimation error on time reversal UWB communication system," *Wireless Personal Communications*, vol. 68, no. 2, pp. 433–439, 2013.

[37] G. Caso, L. D. Nardis, M. T. P. Le, F. Maschietti, J. Fiorina, and M.-G. D. Benedetto, "Performance evaluation of non-prefiltering vs. time reversal prefiltering in distributed and uncoordinated IR-UWB ad-hoc networks," *Mobile Networks and Applications*, vol. 22, no. 5, pp. 796–805, 2017.

[38] P. Setlur and N. Devroye, "An information theoretic take on time reversal for nonstationary channels," *IEEE Signal Processing Letters*, vol. 20, no. 4, pp. 327–330, 2013.

[39] U. Zia, I. H. Naqvi, and M. Uppal, "Performance of ultra-wideband timereversal systems under imperfect channel side information at the transmitter," *IEEE Electronics Letters*, vol. 51, no. 7, pp. 585-586, 2015.

[40] U. Zia, M. Uppal, and I. H. Naqvi, "Robust feedback design for time reversal UWB communication systems under CSIT imperfections," *IEEE Communications Letters*, vol. 19, no. 1, pp. 102–105, 2015.

[41] X. Wang and J. Wang, "Effect of imperfect channel estimation on transmit diversity in CDMA systems," *IEEE Transactions on Vehicular Technology*, vol. 53, no. 5, pp. 1400–1412, 2004.

[42] G. Caire, N. Jindal, M. Kobayashi, and N. Ravindran, "Multiuser MIMO achievable rates with downlink training and channel state feedback," *Institute of Electrical and Electronics Engineers Transactions on Information Theory*, vol. 56, no. 6, pp. 2845–2866, 2010.

[43] J. Fiorina, G. Capodanno, and M.-G. Di Benedetto, "Impact of time reversal on multi-user interference in IR-UWB," in *Proceedings of the 2011 IEEE International Conference on Ultra-Wideband, ICUWB 2011*, pp. 415–419, September 2011.

[44] E. G. Larsson and P. Stoica, *Space-Time Block Coding for Wireless Communications* , Cambridge University Press, Cambridge, UK, 2003.

[45] D. V. Sarwate and M. B. Pursley, "Correlation properties of pseudo random and related sequences," *Proceedings of the IEEE*, vol. 68, no. 5, pp. 593–619, 1980.

[46] A. Mitra, "On pseudo-random and orthogonal binary spreading sequences," *International Journal of Electrical, Computer, Energetic, Electronic and Communication Engineering*, vol. 2, no. 12, pp. 2836–2843, 2008.

[47] E. Biglieri, *Coding for Wireless Channels*, Springer, 2005.

[48] J. Foerster, "Channel modeling subcommittee report (final)," in *Proceedings of the IEEE P802.15.3a Working Group, P802.15-03/02490r1-SG3a*, 2003.

[49] J. Fiorina and D. Domenicali, "The non validity of the gaussian approximation for multi-user interference in ultra wide band impulse radio: from an inconvenience to an advantage," *IEEE Transactions on Wireless Communications*, vol. 8, no. 11, pp. 5483–5489, 2009.